

The Electrical Soil Heating Preheat Phase of Dynamic Underground Stripping

Contents

Abstract.....	3-137
Introduction & Background	3-138
Theory of Electrical Heating.....	3-140
Experimental Setup	3-143
Results & Discussion	3-145
Energy Balance Above the Water Table.....	3-146
Energy Balance Below the Water Table.....	3-150
Additional Changes due to Electrical Heating.....	3-150
Conclusions	3-151
Acknowledgments	3-151
References.....	3-152
List of Figures	3-154
Appendix A: The Relative Importance of Joule and Conduction Heating	3-171
Appendix B: Time History of Energy Deposition for Individual Electrodes	3-175

The Electrical Soil Heating Preheat Phase of Dynamic Underground Stripping

**H. Michael Buettner
William D. Daily**

Abstract

Powerline-frequency electric currents were used in an electrical preheating phase prior to steam injection and vacuum extraction for cleanup of a gasoline spill at the Lawrence Livermore National Laboratory (LLNL). The goal of the electrical preheating was to raise the temperature of the contaminated clay units as close to the boiling point of water as possible thus vaporizing the gasoline and causing it to move into the permeable clay units via pressure gradients where it would be removed by subsequent steam injection and vacuum extraction. This work began in November of 1992 and ended in early January, 1993.

Some 202,000 kW · h of electrical energy was deposited in the soil by a system of 11 electrodes, 3 above the water table, and 8 below. The power distribution system was capable of delivering 60 Hz, 3-phase power at voltages of 208, 350, 480, and 600 volts ac (Vac), and had a total capacity of 1500 kV · A. The average power dissipated during heating was 434 kW and the maximum was 980 kW. Individual heating wells operated above 100 kW.

About 55,000 kW · h of the total energy was deposited above the water table in a 15 m-thick zone whose volume was approximately 6500 m³, and temperature increases ranged from a few °C to over 70 °C in various temperature monitoring wells. An energy balance for the upper zone is consistent with known soil properties, temperature increases and the energy input.

The remaining 147,000 kW · h of energy was deposited below the water table in a 10-m thick zone whose volume was about 11,700 m³, and temperature increases ranged from a few °C to about 20 °C in the temperature monitoring wells.

Total fuel hydrocarbon levels in three nearby monitoring wells increased from their historical values of around 25,000 ppb before electrical heating to around 150,000 ppb after heating, indicating that free-phase gasoline was being mobilized in the vicinity.

Introduction & Background

Electrical heating of soil is not a new idea. Both powerline-frequency (60 Hz) and radio-frequency (in the HF range of 3 to 30 MHz) heating have been used in the oil industry to reduce the viscosity of the bitumen to the point where oil can be recovered from the formation. Chute and Vermeulen (1988) present a survey of laboratory and field applications of electromagnetic reservoir heating. They conclude that, in general, powerline-frequency methods are preferable to radio-frequency methods when 1) the desired temperatures are lower than the *in-situ* boiling point in the soil, and 2) when the formation contains sufficient water so that electrical resistances between heating wells are low enough to permit acceptable heating rates at applied voltages of less than a few thousand volts.

In contrast, radio-frequency induction methods should be considered when 1) the formation is to be heated to temperatures above the *in-situ* steam temperature, and/or 2) where the formation contains very little initial moisture. However, there can be substantial capital costs associated with the conversion of powerline-frequency energy to radio-frequency energy. In simple terms, 1 watt of 60 Hz power is much cheaper than 1 watt of radio-frequency power. Additionally, 60 Hz power transmission and distribution equipment is much easier and cheaper to maintain.

The idea of applying electrical soil heating to *in situ* hazardous waste remediation is relatively recent. It relies on the fact that the vapor pressure for many liquid organic compounds increases markedly with temperature. In general, the relation between vapor pressure and temperature can be expressed as

$$\log p = b - [0.05223 a / (T + 273)]$$

where p is the pressure in mm of mercury of the saturated vapor, T is the temperature in degrees Celsius, and a and b are empirical constants. Figure 1 shows the relationship for a few compounds of interest (Weast, 1989). Though one cannot use this relationship alone to calculate vapor pressures in contaminated soil because of the effects of surface tension, water solubility and sorption on solid surfaces, the data of Figure 1 strongly suggest that increasing the temperature of soil should increase the volatility of organic contaminants thus making them easier to remove.

Powerline-frequency electrical heating methods for remediation of VOCs in soil and ground water are known to be under investigation by two groups in the United States. Electrical soil heating was successfully demonstrated first at LLNL in the field on an engineering-scale (89 m³ target volume) in September of 1991 (Buettner et al., 1992 and Aines et al., 1992).

Workers at Pacific Northwest Laboratory (PNL) have also demonstrated electrical soil heating. Heath et al. (1992) demonstrated electrical soil heating on a laboratory scale (1.13 m³ volume), and this was followed by an engineering-scale (89 m³ target volume) field experiment performed by Bergsman et al. (1993). The soil was uncontaminated in all of the experiments referred to above.

The first known engineering-scale (89 m³ target volume) field test of powerline-frequency electrical heating in combination with vacuum venting for remediation of VOCs was performed by LLNL in August of 1992 (Buettner et al., 1993). This field test was performed on soil contaminated by trichloroethylene at LLNL's Site 300, about 15 miles east of the main site.

As discussed in this paper, electrical soil heating has been combined with steam injection and vacuum venting in a process known as Dynamic Underground Stripping. This technique was applied to the problem of cleaning gasoline from soil and groundwater at LLNL. The steam drives contaminated water toward extraction wells. Volatile organic compounds are distilled from the hot soil and moved to the steam/groundwater interface, where they condense and are pumped to the surface. Vacuum extraction continues to remove residual contaminants.

Steam sweeping works very well on the permeable zones (sands and gravels) but not so well on the tight zones (clays and silts) which are heated very slowly by conduction or missed entirely. The role of electrical soil heating is to target these clay zones which are unaffected by steam.

In Dynamic Underground Stripping, it was intended that electrical soil heating be used in a preheat mode prior to steam injection, and after steaming to target the zones missed by steam. The rationale behind the preheating was that the electrical conductivity contrast between the gravel and clay zones should be maintained. That is, the clay zones which are more conductive at the start, should stay more conductive throughout the process. This is desirable since subsequent current flow (and heating) will be concentrated in the more electrically conductive zones. The electrical preheat process increases the conductivity of the soil through an increase in ionic conductivity, and calculations at LLNL (Chesnut, 1992) indicate that a 20 °C preheat is sufficient to keep the conductivity of the clay zones at a value larger than that of the gravel zones.

Theory of electrical heating

Electrical or joule heating is conceptually very simple. When electric currents flow through soil, power will be dissipated through ohmic losses, and this is manifested by heating of the soil. This process is analogous to the operation of the heating element in a simple home space heater or the heating element of an electric range. If one chooses to use powerline frequency heating, then power sources are readily available from the commercial power grid or motor-generators.

The simple theory for electrical heating is described below. This analysis is confined to the case of a two-dimensional model with homogenous electrical and thermal properties. The effects of phase changes and fluid flow through the soil are ignored.

Expected initial heating rates are based on solutions to the heat equation

$$\frac{\partial T}{\partial t} = \frac{k}{c_p} \nabla^2 T + \frac{U}{c_p} \quad (1)$$

where T is the temperature ($^{\circ}\text{C}$), k is the thermal conductivity ($\text{joule} / \text{m} \cdot ^{\circ}\text{C} \cdot \text{s}$), c is the specific heat ($\text{joule} / \text{kg} \cdot ^{\circ}\text{C}$), ρ is the soil density (kg / m^3), and U is the heat source term (W / m^3). The source term is given by

$$U = \sigma |\bar{E}|^2 \quad (2)$$

where σ is the electrical conductivity (S / m) and \bar{E} is the electric field (V / m). The electric field is found from the gradient of the electric potential, $V(x,y)$, which is the solution to Laplace's equation. It is not difficult to show that the solution in two dimensions for line source currents has the form:

$$V(x,y) = -(2\pi\sigma)^{-1} [\pm I_1 \ln(r_1) \pm I_2 \ln(r_2) \cdots \pm I_n \ln(r_n)] \quad (3)$$

where I_i is the current per unit length at the i th location, the positive sign is assigned to current sources, the negative sign to current sinks, and r_i is the distance from some observation point (x,y) to the source or sink at the i th location.

Calculations of the heating rate are for early time when the first term on the right-hand side of equation (1) is small compared to the second. When the current is first turned, on this will be true, since the temperature distribution is uniform ($\nabla^2 T = 0$). In early time, then, the temperature will vary linearly with time according to

$$T = T_0 + \frac{U}{c\rho} \Delta t \quad (4)$$

where T_0 is the starting temperature and Δt is the elapsed time. Even at later times, the linear relationship can hold provided that the "Laplacian" term of equation (1) remains small compared to the heat source term. The validity of this assumption can be tested by examining the time behavior of the temperature readings for linearity.

The simple, 2-dimensional model has been verified by comparison to results from earlier LLNL work at an uncontaminated site (Buettner, et al., 1992). In this field

demonstration, six heating wells were placed as shown in the plan view of Figure 2. Temperatures were monitored in wells TEP-SNL-012, TEP-SNL-013, HW-SNL-056, and HW-SNL-056. Heating rates were measured during the first 10 days of this demonstration when heating took place 24 h/day. The values used in the model calculations were: 1) current per electrode of 12 A/m, 2) radius of the heating well pattern of 3.05 m, 3) electrode length of 3.05 m, 4) soil electrical conductivity of 0.1 S/m, and 5) soil volumetric heat capacity of $2 \times 10^6 \text{ joule/}^\circ\text{C} \cdot \text{m}^3$ (Carslaw and Jaeger, 1959). The measured and calculated (in brackets) rates for the four wells above during the first 10 days were 1.60 [2.27] $^\circ\text{C} / \text{day}$, 2.89 [3.74] $^\circ\text{C} / \text{day}$, 2.27 [2.37] $^\circ\text{C} / \text{day}$, and 4.65 [4.09] $^\circ\text{C} / \text{day}$ respectively. Given the simplicity of these calculations, the agreement is quite good.

The reader will note that owing to the form of the electrical potential from Equation (3), that the electric field varies as r^{-1} and the corresponding heating rate, U/cp , will vary as r^{-2} . The result is a rapid decrease in heating rate as one moves away from an electrode. This drop off in heating rate as a function of distance is even more pronounced for the point-source electrode case where the electrical potential varies as r^{-1} , the electric field varies as r^{-2} , and the heating rate varies as r^{-4} . In practice, for the finite-sized electrode case, the actual heating rate will vary between r^{-2} and r^{-4} .

The above 2-dimensional analysis is applicable to homogeneous media with line current sources. In practice, it may also be applied when the geometry is nearly 2-dimensional. For example, it can be applied to the case of electrodes whose length is comparable to the electrode spacing. It may also be applied to the case of electrodes embedded in a highly-conductive layer which is bounded above and below by highly-resistive layers. In the experiments described here, the geometry is not truly 2-dimensional, and the previous results will not apply exactly. This will be discussed further in a subsequent section. For a discussion of more realistic 3-dimension models, the reader is referred to the chapter by Carrigan (1994).

The simple analysis above also neglects heating by conduction. Heating by conduction can be important as well, particularly well away from heating electrodes. See Appendix A for a simple analysis comparing joule heating to conductive heating.

Experimental setup

A plan view of the Gas Pad site is shown in Fig. 3. Note that there are four different types of wells at this site. The GIW wells combine steam injectors with electrodes for soil heating and surround the bulk of the spill. The electrodes in these wells target the lower clay unit at and below the water table. The HW wells are for electrical heating only and have separate electrodes in both the upper and lower clay units. The TEP wells are thermocouple monitoring wells. Finally, the GEW and GSW wells are extraction wells which are located near the center of the pattern. Details of the well designs and completions can be found elsewhere in this report (Siegel, 1994).

Lithologies for the TEP wells are shown in Fig. 4. Note that there are few well-defined, continuous units which intersect all the TEP wells. However, there is a clay-rich unit near and below the water table, with a sandy/gravelly unit below (the lower permeable zone), and silty/sandy/gravelly units above (the upper permeable zone). Other clay-rich units occur at shallower depths. The heating strategy is to employ steam in each permeable zone and electrical heating in each impermeable zone.

The configuration of electrodes was chosen to work in concert with the steam injection wells. Thus, 5 electrodes were placed in the clay zones between the two permeable steam-injection zones (below the water table) in wells GIW-813, 814, 815, 818, and 819. These wells were placed far enough apart to surround the bulk of the gasoline spill below the water table. These wells also had steam injectors in the permeable units above the water table.

Six additional electrodes were placed in wells HW-001, 002, and 003 which were located closer to the center of the spill. Three of these electrodes were in the clay units below the water table, while the other three were placed in clay units in the contaminated vadose zone.

The electrical heating system derives its power from the LLNL grid. A block diagram of the power distribution system can be found in the Engineering section of this report (Siegel, 1994). Power is supplied from the grid at 13.8 kV and applied to the primary side of a 1500 kV · A transformer by means of a 15 kV, 600

A load interrupter switch. The working voltages on the secondary side of the transformer are 208, 350, 480, and 600 Vac, 60 Hz, three-phase. These voltages were chosen to offer some degree of control over the electrode currents. The lowest value was selected to account for the lowest inter-electrode resistance we expected to encounter, while the highest value was chosen because it was the highest practical voltage we could use without resorting to special high voltage equipment and safety requirements.

The secondary voltage is switched ON or OFF by the main circuit breaker (5000 Amps, 600 Vac, 3 pole) and transmitted by a wireway to a low voltage switchboard. The switchboard contains 12 adjustable trip breakers (one per heating electrode), and it is at this switchboard where the appropriate secondary voltage and phase are assigned to each electrode. The detailed specifications of the electrical system may be found in the Engineering section of this report (Siegel, 1994).

During the course of the electrical preheating portion of Dynamic Underground Stripping, two electrode phasing configurations were used. The first of these, the baseline configuration, was used from November 11, 1992 to November 24, and then from December 1 to January 6, 1993. The phasing arrangement and primary current flow paths are shown in Fig. 5. This results in current flow paths which break the overall pattern into the smallest possible triangles.

From November 24 to December 1 the alternate phasing configuration of Fig. 6 was used. The idea behind this configuration was to group adjacent electrodes by phase. For example, the four electrodes in GIW 818, 819, and HW-002 were all connected to phase A, and there would be no current flow between them. By eliminating some of the peripheral flow paths as compared to the baseline configuration, we hoped to deposit more of the energy inside the pattern.

Safety was an important consideration during electrical heating operations. The Gas Pad site is adjacent to LLNL's shipping and receiving yard, a busy truck gate, an employee parking lot, and a county road. An extensive safety review was conducted and an operational safety procedure (OSP) was written to formalize the safety requirements. In brief, the main controls were 1) operation was to occur only at night so that few people would be in the area, 2) the area containing all the

heating and steam injection wells was fenced and made into a keep-out zone protected by interlocks during electrical heating, and 3) step and touch potentials measured outside the fenced area and were constrained to be 10 Vac or less. The controls outlined in the OSP were derived from prior experience at LLNL's Clean Site experiment (Aines et. al., 1992) and consultation with the LLNL Hazards Control Department. Additional details of the safety requirements can be found in the Engineering section of this report (Siegel, 1994).

Results & Discussion

From an efficiency point of view it is not desirable to heat sand and gravel units with electricity. Thus, electrical current flow should be confined to the clay units as much as possible. To accomplish this, the clay units should always be more electrically conductive than the more permeable sand and gravel units. When this is the case, current will flow preferentially in the clay units and tend to stay out of the sand and gravel zones. This situation is preferred since the electrical heating is intended to heat the clay zones while steam heats the sand and gravel zones.

Initially, the clay units are more electrically conductive than the sand and gravel units. However, the electrical conductivity of partially saturated soils increases with temperature. Thus it is possible for the conductivity of the sand and gravel units to increase sufficiently so that it is comparable to that of the clays. Preheating the clays should prevent this situation. Calculations made at LLNL (Chesnut, 1992) indicate that a 20 °C preheat of the clays should raise their conductivity to a value great enough so that they will always be more conductive than the sands and gravels.

The electrical preheat goal was to achieve at least a 20 °C temperature increase in the clay units prior to the onset of steam injection. Calculations showed that a 20 °C increase was possible in a period of about 8 weeks.

Electrical soil heating began on November 11, 1992 with the baseline phasing configuration of Fig 5. The starting secondary voltage was 208 Vac. Our working strategy was to begin with the lowest voltage and carefully observe the performance of the system before increasing the secondary voltage. The diagnostics consisted of inductive current probes on the feed cables to each

electrode and T-type thermocouples placed on the electrodes and in the temperature monitoring (TEP) wells.

The secondary voltage was increased to 350 Vac on November 16, to 480 Vac on November 23, and finally to 600 Vac on December 14, 1992. The voltage remained at 600 Vac until the heating ended on January 6, 1993.

A plot of the total power versus time during the course of the experiment is shown in Fig. 7. The time is measured in days starting on November 11, 1992. The increases in power when the voltage was increased are evident from the figure. The "OFF" periods take place during the day, during some holidays and weekends, during heavy rain periods, and during maintenance or repair times. Note that the maximum power achieved was some 980 kW and the average power during heating was 434 kW.

The corresponding total energy plot is shown in Fig. 8. This was obtained by integrating the power versus time data. During the course of the experiment some 202,000 kW · h of energy was deposited. Of this amount approximately 55,000 kW · h was deposited above the water table (at about 102 ft) by the upper electrodes in wells HW-GP-001, 002, and 003.

The energy plots for individual wells are shown in Appendix B.

Energy balance above the water table

It is easier to treat the zone above the water table since convective heat flow due to mobile water can be neglected. The upper zone is heated primarily by the upper electrodes in wells HW-GP-001, 002, and 003. An examination of Fig. 3 shows that the heating response in the region around HW-GP-003 is best characterized by monitoring wells TEP-7 and TEP-8. HW-GP-002 has TEP-9 nearby. Finally TEP-10 is at the approximate center of the triangle formed by HW-GP-001, 002, and 003. Unfortunately there is essentially no thermocouple coverage near well HW-GP-001.

A rough estimate of the expected temperature increase in the upper zone can be made as follows. The energy deposited by wells HW-GP-001, 002, and 003 was

21,000 kW·h, 9300 kW·h, and 25,000 kW·h respectively. The area heated by the three wells encompasses the triangle defined by the three wells along with some soil outside the triangle because current flows outside as well. Assuming that Livermore soils have an "average" volumetric heat capacity of $0.56 \text{ kW}\cdot\text{h}/\text{m}^3\cdot^\circ\text{C}$ (Carslaw & Jaeger, 1959), then the total energy input of 55,300 kW·h would result in a volume-temperature product of $98,750 \text{ m}^3\cdot^\circ\text{C}$. Furthermore if the heated zone is assumed to be a cylinder with a height of 15 m and a radius of 11.7 m (the circle which inscribes the three heating wells), then the expected temperature increase would be 15.2°C . This is very close to the preheat goal of 20°C .

The actual results of electrical heating are detailed by the temperature data obtained throughout the field. These data can be used to estimate the electrical heating effects in terms of a volume-temperature product for the heated soil. Temperature logs for wells TEP 7, 8, 9, and 10 are presented in Figs. 10-13 respectively. These logs were made at the end of the electrical heating phase using a tool which employs an infra-red measurement head (Goldman, 1994) and corrected to match fixed thermocouple values at selected depths. It is apparent from Figs 10-13 and the well lithologies of Fig. 4 that the upper clay-rich zone affected by electrical heating extends from about 15 m to 30 m depth.

The first step in the estimate is to integrate the temperature profiles from 15 m to 30 m to obtain a value of the distance-temperature product for the upper electrical heating zone in each well. An electrical heating-induced distance-temperature product is calculated by subtracting the preheating value of $15 \text{ m}\cdot 20.7^\circ\text{C} = 311 \text{ m}\cdot^\circ\text{C}$ from this integral. If the electrical heating-induced distance-temperature product were known for many locations throughout the heated volume, it would be a simple matter to integrate over the area to obtain the total volume-temperature product resulting from electrical heating.

However, the distribution of the temperature monitoring wells, TEP 7, 8, 9, and 10 is rather sparse so some educated guesses about the temperature distributions in other locations are required before the distance-temperature products can be obtained and integrated over the area. To aid in the process of estimating distance-temperature products, a plan view of the region around heating wells HW-001, 002, and 003 is shown in Fig. 14.

In the area around well HW-003, the temperature distribution of well TEP 7 is assumed to apply to a circle of radius 5.18 m. The electrical heating-induced distance-temperature product for TEP 7 is $334 \text{ m}\cdot^{\circ}\text{C}$. This value was obtained by integrating the temperature vs. depth plot of Fig. 10 from 15 m to 30 m and subtracting the pre-electrical heating value of $311 \text{ m}\cdot^{\circ}\text{C}$.

The distance-temperature product for well TEP 8 is $66 \text{ m}\cdot^{\circ}\text{C}$ and applies to a circle of radius 7.62 m around HW-003. To obtain the distribution in HW-003, the temperature distribution is assumed to be similar to that of TEP 7 from a depth of 15 m to the top of the electrode, and from the bottom of the electrode to a depth of 30 m. Over the length of the electrode the temperature is assumed to be 100°C . This results in a distance-temperature product of $451 \text{ m}\cdot^{\circ}\text{C}$. The assumption of 100°C temperature at the electrode should be good because ground water is boiling at the electrodes. In reality the temperature values above and below the electrode will be greater than the corresponding values in TEP 7, and using the values from TEP 7 will result in an underestimate of the distance-temperature product.

The same procedure is used to estimate distance-temperature products around heating well HW-001. This is done because the nearest temperature monitoring well, TEP 10, is far away, wells HW-003 and HW-001 have nearly identical time histories for deposited energy (see Appendix B), and because wells HW-003 and HW-001 have nearly equal total deposited energies-- $25,000 \text{ kW}\cdot\text{h}$ and $21,000 \text{ kW}\cdot\text{h}$ respectively.

Around well HW-002 the distribution of TEP 9 is assumed to apply to a circle of radius 3.66 m, resulting in a distance-temperature product of $81 \text{ m}\cdot^{\circ}\text{C}$. The distribution in well HW-002 is assumed to be like TEP 9 from 15 m to the top of the electrode, 100°C over the electrode, and like TEP 9 from the bottom of the electrode to 30 m. The distance-temperature product for HW-002 is $300 \text{ m}\cdot^{\circ}\text{C}$.

To complete the analysis, the distance-temperature products must be calculated at some other locations to fill in the missing parts of the heated volume. The plan view of Fig. 14 shows the circles around each of the three wells with their corresponding distance-temperature products. There are three circles with an

associated distance-temperature product of $28 \text{ m} \cdot ^\circ\text{C}$, and the procedure used to arrive at this value is described below.

Equal-radius circles from HW-001 and 003 which just touch have a radius of 10.7 m. Linear interpolation along the direction of straight lines drawn from TEP 10 to HW-001 and 003 is used to estimate the distance-temperature product on each of the 10.7 m circles. Since the distance-temperature products on the 7.62 m circles and at TEP 10 are $66 \text{ m} \cdot ^\circ\text{C}$ and $17 \text{ m} \cdot ^\circ\text{C}$ respectively, linear interpolation yields values of $31 \text{ m} \cdot ^\circ\text{C}$ on the 10.7 m circle from HW-003 and $25 \text{ m} \cdot ^\circ\text{C}$ on the 10.7 m circle from HW-001. To normalize the distribution, the average value of $28 \text{ m} \cdot ^\circ\text{C}$ is used for both circles. A circle from HW-002 which just touches the 10.7 m circle from HW-003 is also assigned a value of $28 \text{ m} \cdot ^\circ\text{C}$.

The volume-temperature product for each of the regions of Fig. 14 is now computed using the values shown in Fig. 14 and assuming that the volume-temperature product varies linearly between concentric circles. The result of this process is a total volume-temperature product of $138,000 \text{ m}^3 \cdot ^\circ\text{C}$. Given the assumptions that have been made, this value is reasonably close to the value of $98,750 \text{ m}^3 \cdot ^\circ\text{C}$ obtained earlier in this section. Note that a small portion of the area around TEP 10 is omitted in this estimate, however, its value would not exceed about $28 \text{ m} \cdot ^\circ\text{C} \times 60 \text{ m}^2 = 1700 \text{ m}^3 \cdot ^\circ\text{C}$ so it can be neglected.

Using the distance-temperature products derived for the region around heating well HW-003, a test of the simple 2-dimensional model is possible. Assume that the heating in wells TEP 7 and 8 is due primarily to the energy deposited by HW-003. Based on the results of the theory section of this report it, is easy to show that the electric field due to a line electrode is given by $\frac{(I/l)}{2\pi r\sigma}$ where σ is the electrical conductivity of the soil, I/l is the current per unit length of electrode, and r is the radial distance from an observation point to the electrode. The heating rate is given by $\frac{1}{\sigma(cp)} \left(\frac{(I/l)}{2\pi r} \right)^2$ where cp is the volumetric heat capacity. Integration of the heating rate over the course of the experiment should then yield the temperature increase. The following values were used for the calculation: 1) electrical conductivity of 0.1 S/m , 2) volumetric heat capacity of $2 \times 10^6 \text{ joule}/^\circ\text{C} \cdot \text{m}^3$, 3) 1

= 3.05 m, and 4) $r = 5.18$ m (for TEP 7) and 7.62 m (for TEP 8). Using these values and integrating the measured values of I^2 over the course of the electrical preheat, results in temperature increases of 32.1 °C and 14.8 °C for TEP 7 and 8 respectively. Recalling that the distance-temperature product for TEP 7 was 334 m°C, and that the thickness of the heated region was 15 m, the temperature rise should be 22.3 °C. Similarly for TEP 8, the distance-temperature product was 66 m°C, and the temperature rise should be 4.4 °C. The degree of agreement is good at 5.18 m and not so good at 7.62 m. Many factors can account for the discrepancy. Some of them are: 1) the actual heating distribution will be strongly controlled by soil heterogeneities, which have been neglected, 2) the values used for the soil thermal and electrical properties are estimates only, 3) a full, 3-dimensional treatment should be used.

Energy balance below the water table

Some 147,000 kW·h of energy was deposited below the water table. Assuming an average soil with a 30% porosity, the volumetric heat capacity would be around 0.74 kW·h/m³·°C, resulting in an expected volume-temperature product of about 199,000 m³·°C. Below the water table, the heated zone is defined by the electrodes in wells GIW-813, 814, 815, 818, 819 and the lower electrodes in wells HW-001, 002, and 003. The lower bound on the area of the heated zone is defined by the polygon whose vertices are wells GIW-813, 814, 815, 818, 819, and HW-001. The effective heated area is larger than the polygon (1169 m²) because heated water is free to move around and currents flow outside the polygon too. Assuming that the heated area is twice that of the polygon or 2338 m² and that the thickness of the heated region is 10 m, the total volume is 23380 m³. The expected temperature rise is 8.5 °C. This value seems representative of the temperature logs for the lower zone (Figures 10-13).

Additional changes due to electrical heating

Electrical heating was apparently responsible for an increase in total fuel hydrocarbon levels in ground water, as evidenced by the increased concentrations in wells GSW-006, GSW-001A and GEW-710 (Fig. 9). Historical concentrations of around 25,000 ppb were present for several years before heating and rose to around 150,000 ppb after heating. These data add credence to the added value of

electrical heating by providing information in areas not covered by thermocouple wells.

Conclusions

Powerline-frequency electric current can be used effectively to heat soils. The technique appears to work best above the water table, though heating below the water table is possible. Below the water table, the heating effect can be reduced by the movement of mobile water.

Temperatures in various monitoring wells increased by as much as 70 °C to as little as a few °C. An energy balance for the region above the water table was consistent with known soil properties, temperature increases, and energy input. A detailed energy balance was not possible below the water table because the temperature data were too sparse in this region. However, the observed temperature increases in the available monitoring wells were consistent with the assumed soil properties and energy input.

Heating rates are highest near the electrodes and drop off rapidly between electrodes. If the electrodes are placed too far apart, heating well away from the electrodes will take place by a combination of direct electrical heating and by conduction and the rates can be low. The best results from direct electrical heating will take place when electrodes are no more than about 10 m apart, though the exact distance will depend on the details of the electrode configuration, phasing, and site characteristics. In practice, this may mean arraying a larger number of simple, cheap electrodes rather than a small number of complicated and expensive electrodes.

Acknowledgments

This work was supported by the U. S. Department of Energy, Office of Technology Development, EM-50.

References:

1. F. S. Chute, and F. E. Vermeulen, "Present and Potential Applications of Electromagnetic Heating in the *In-Situ* Recovery of Oil", *AOSTRA Journal of Research*, 4(1), 1988.
2. R. C. Weast, editor, *CRC Handbook of Chemistry and Physics*, 70 th Edition, 1989-1990.
3. H. M. Buettner, W. D. Daily, and A. L. Ramirez, "Enhancing Cyclic Steam Injection and Vapor Extraction of Volatile Organic Compounds in Soils with Electrical Heating", Lawrence Livermore National Laboratory, UCRL-ID-109424, March 1992.
4. R. D. Aines, R. L. Newmark, W. A. McConachie, K. S. Udell, D. W. Rice, A. L. Ramirez, W. H. Siegel, H. M. Buettner, W. D. Daily, P. W. Krauter, E. N. Folsom, A. J. Boegel, and D. J. Bishop, "Dynamic Underground Stripping Demonstration Project Interim Progress Report, 1991", Lawrence Livermore National Laboratory, UCRL-ID-109906, 1992.
5. W. O. Heath, J. S. Roberts, D. L. Lessor, and T. M. Bergsman, "Engineering Scaleup of Electrical Soil Heating for Soil Decontamination", *Proc. Nuclear and Hazardous Waste Management, Spectrum '92*, 1992.
6. T. M. Bergsman, J. S. Roberts, D. L. Lessor, and W. O. Heath, "Field Test of Six Phase Heating and Evaluation of Engineering Design Code", *Proc. Nuclear and Hazardous Waste Management, Spectrum '93*, 1993.
7. H. M. Buettner and W. D. Daily, "Cleaning Contaminated Soil Using Electrical Heating and Air Stripping", submitted to the *Journal of Environmental Engineering*, August 1993.
8. D. Chesnut, Lawrence Livermore National Laboratory, private communication, 1992.
9. W. H. Siegel, 1994.

10. H. S. Carslaw and J. C. Jaeger, Conduction of Heat in Solids, Oxford University Press, 1959.
11. Goldman, 1994.
12. R. Aines, 1994.

List of Figures

- Fig. 1 Vapor pressure versus temperature for some volatile organic compounds of interest.
- Fig. 2 Plan view of the well layout at an earlier LLNL field test at an uncontaminated site.
- Fig. 3. Plan view of the well layout at the LLNL gasoline spill site.
- Fig. 4. Lithology logs for the temperature monitoring (TEP) wells at the LLNL gasoline spill site.
- Fig. 5. Phase assignments and primary current flow paths for the baseline electrical heating configuration, November 11-24, 1992 and December 1-January 6, 1993.
- Fig. 6. Phase assignments and primary current flow paths for the alternate electrical heating configuration, November 24, 1992-December 1, 1992.
- Fig. 7. Electrical power vs. time for electrical soil heating at the LLNL gasoline spill site.
- Fig. 8. Total electrical energy vs. time for electrical soil heating at the LLNL gasoline spill site.

Fig. 9. Total fuel hydrocarbon levels before and after electrical soil heating at the LLNL gasoline spill site.

Fig. 10. Temperature profile in well TEP 7 at the end of electrical heating.

Fig. 11. Temperature profile in well TEP 8 at the end of electrical heating.

Fig. 12. Temperature profile in well TEP 9 at the end of electrical heating.

Fig. 13. Temperature profile in well TEP 10 at the end of electrical heating.

Fig. 14. Plan view of upper zone heating wells with estimates of distance-temperature product and circles of influence.

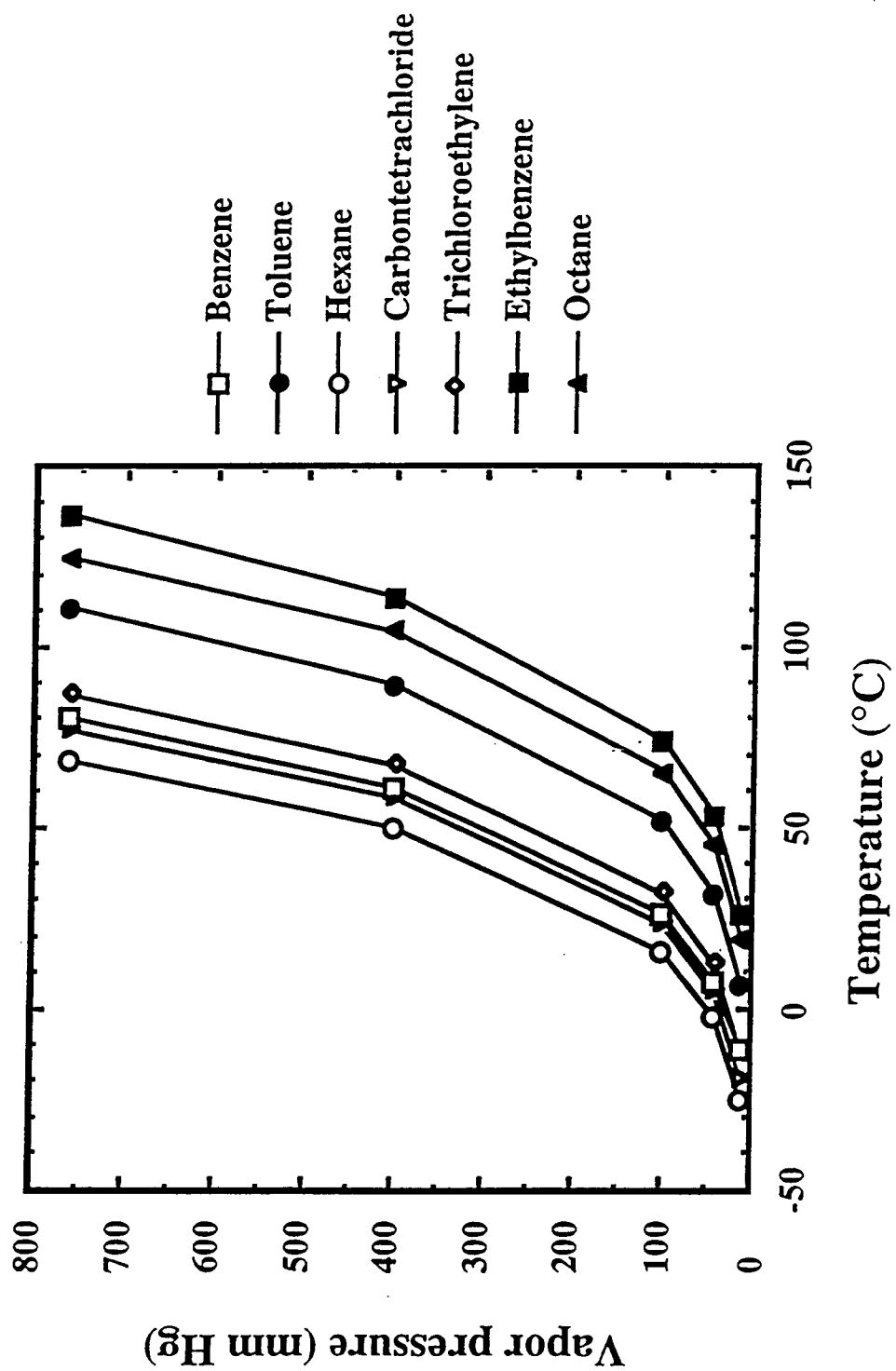


Fig. 1

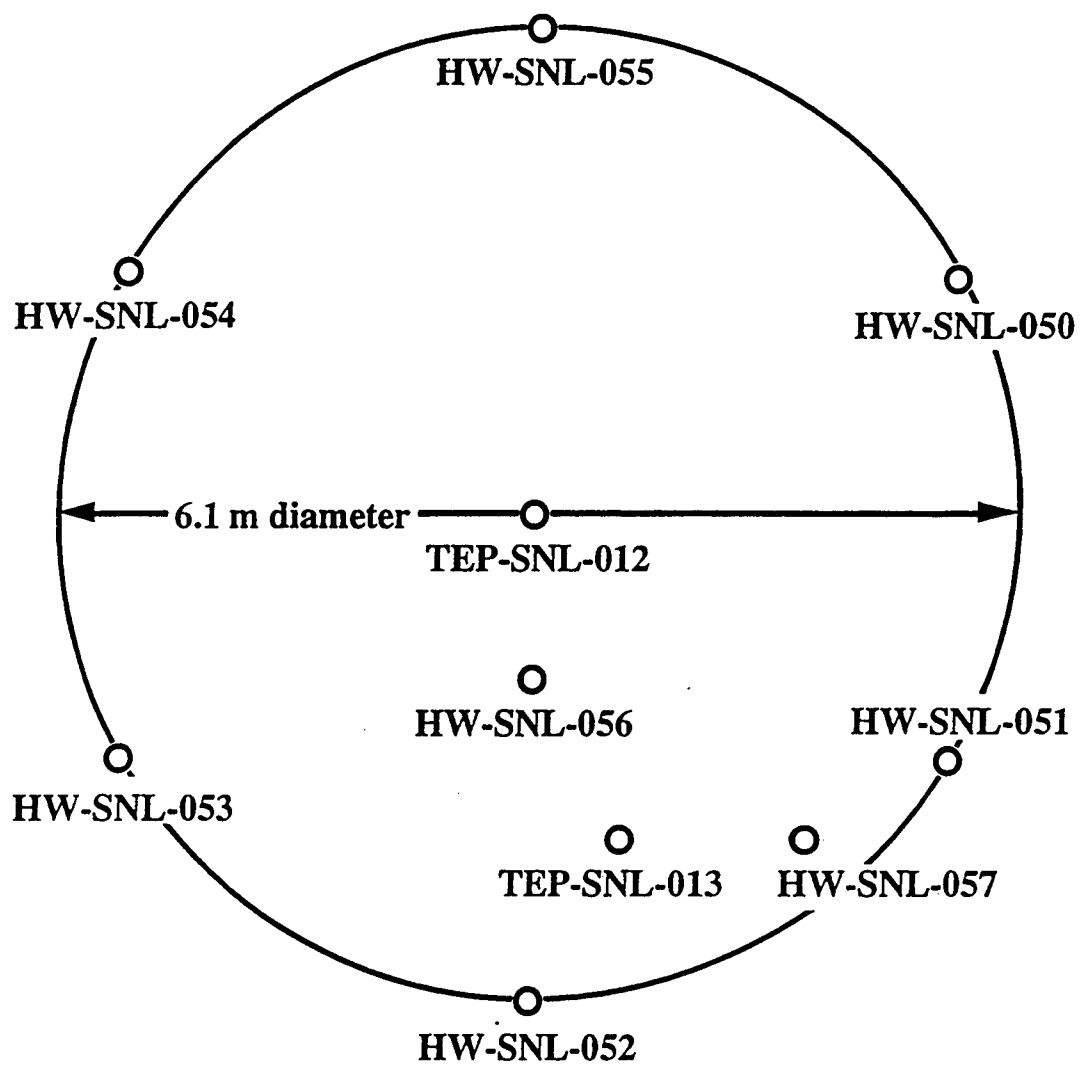
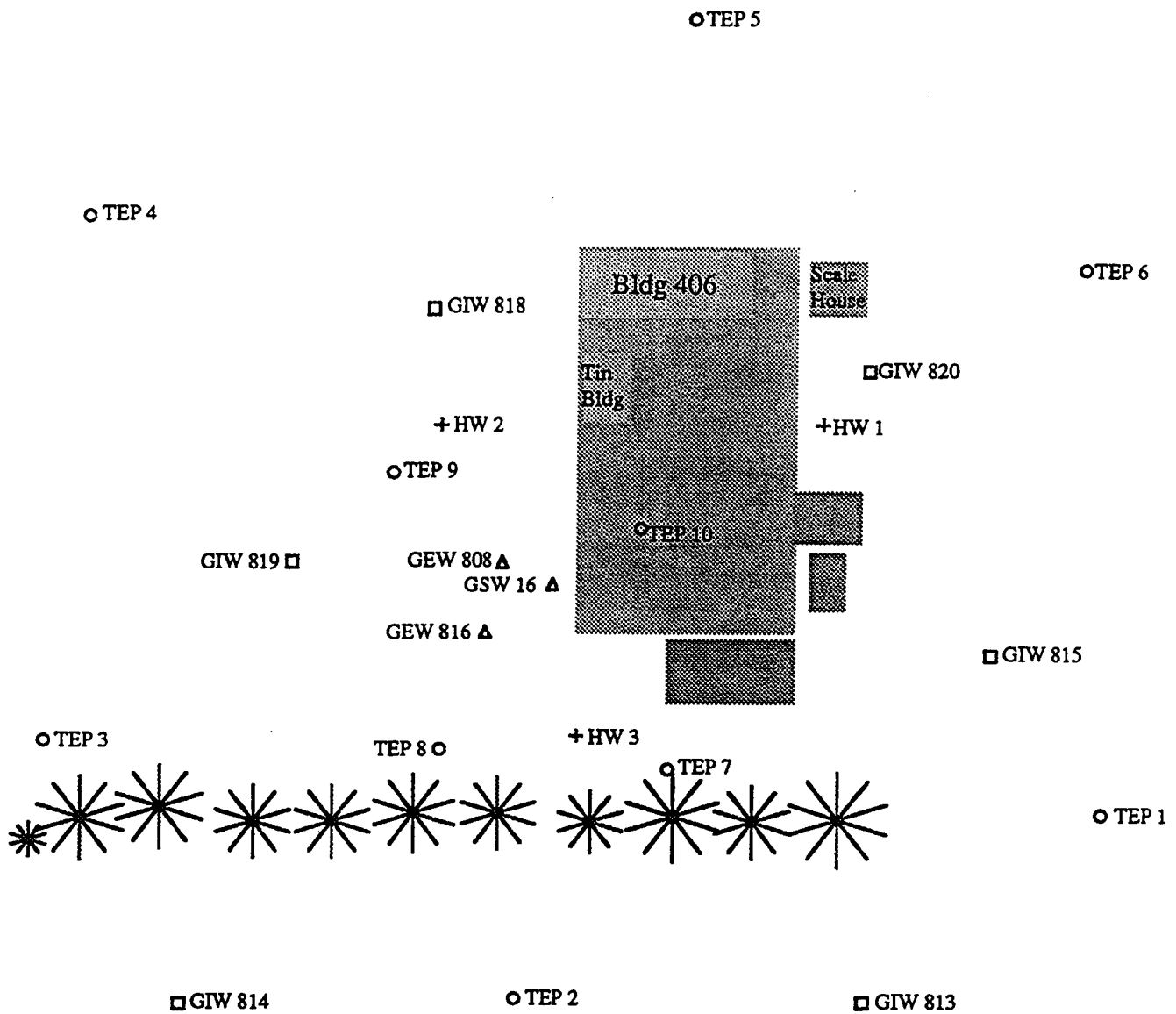


Fig. 2

Dynamic Stripping Project Gas Pad Area



○ TEP 11

Fig. 3

Lithology Images for Gaspad

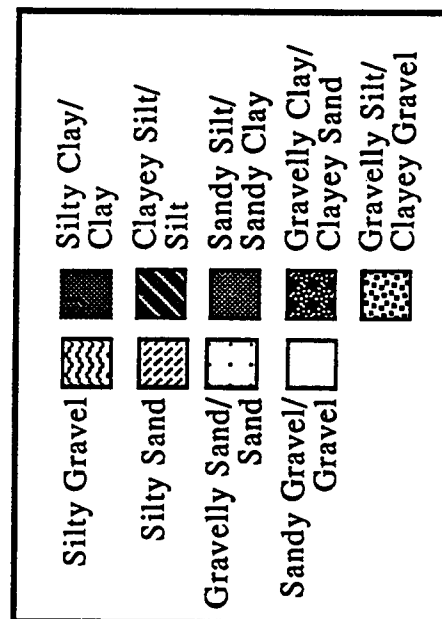
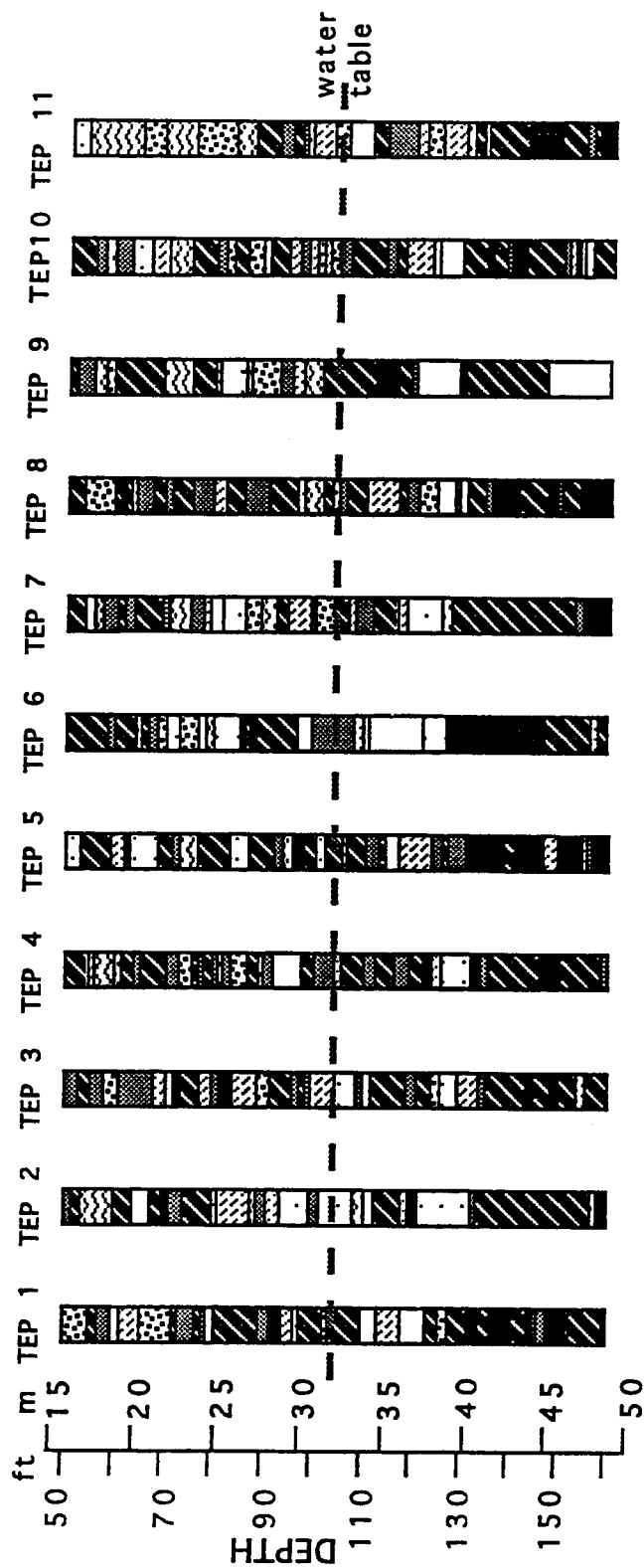


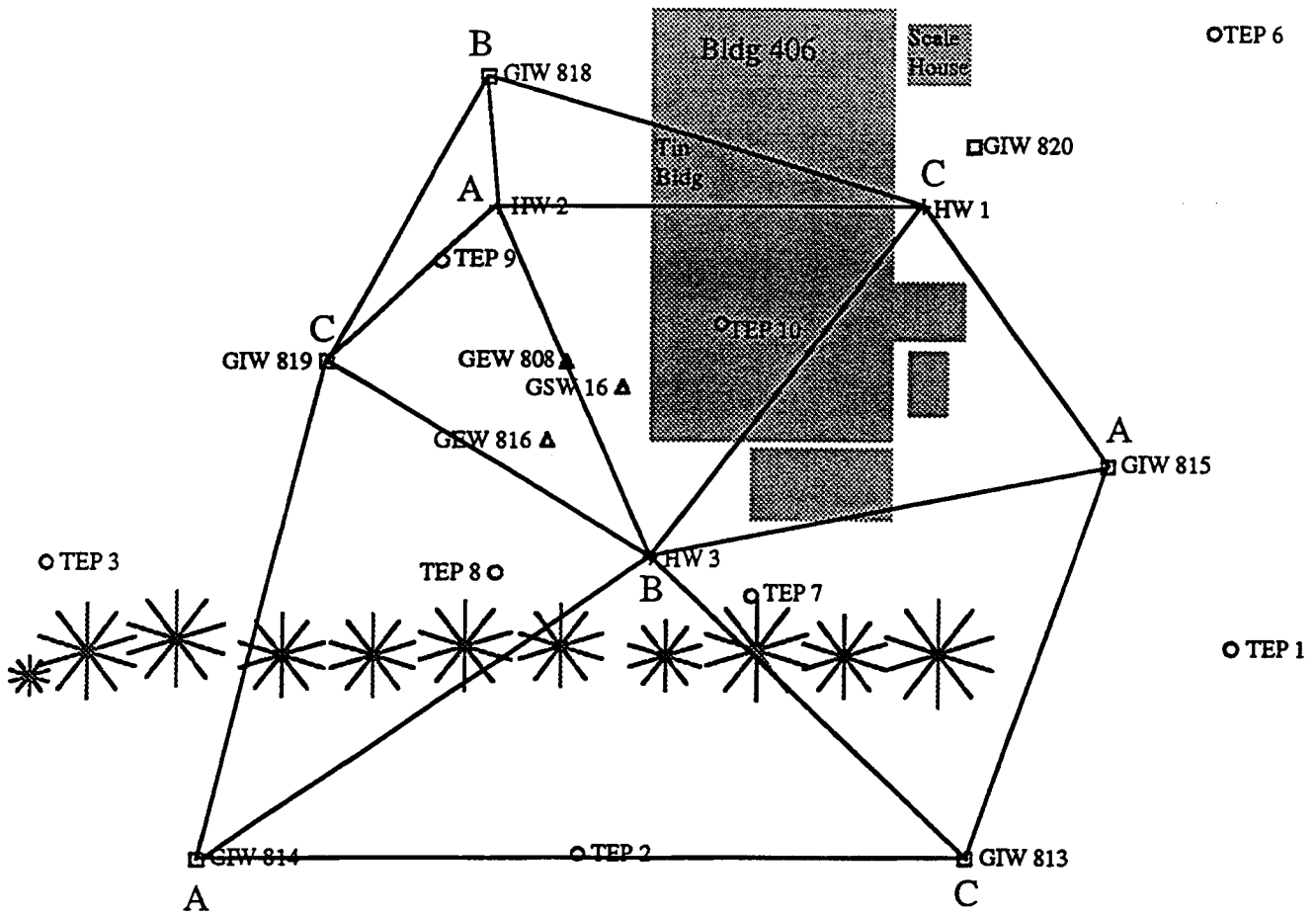
Fig. 4

Dynamic Stripping Project Gas Pad Area

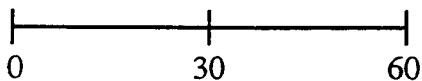
○ TEP 5

○ TEP 4

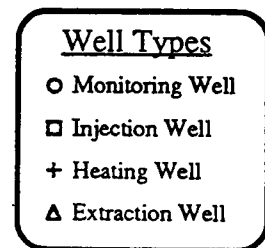
○ TEP 6



Phase assignments and primary current flow paths
for baseline electrical heating configuration, Nov 11-24
and Dec 1-Jan 6 '93



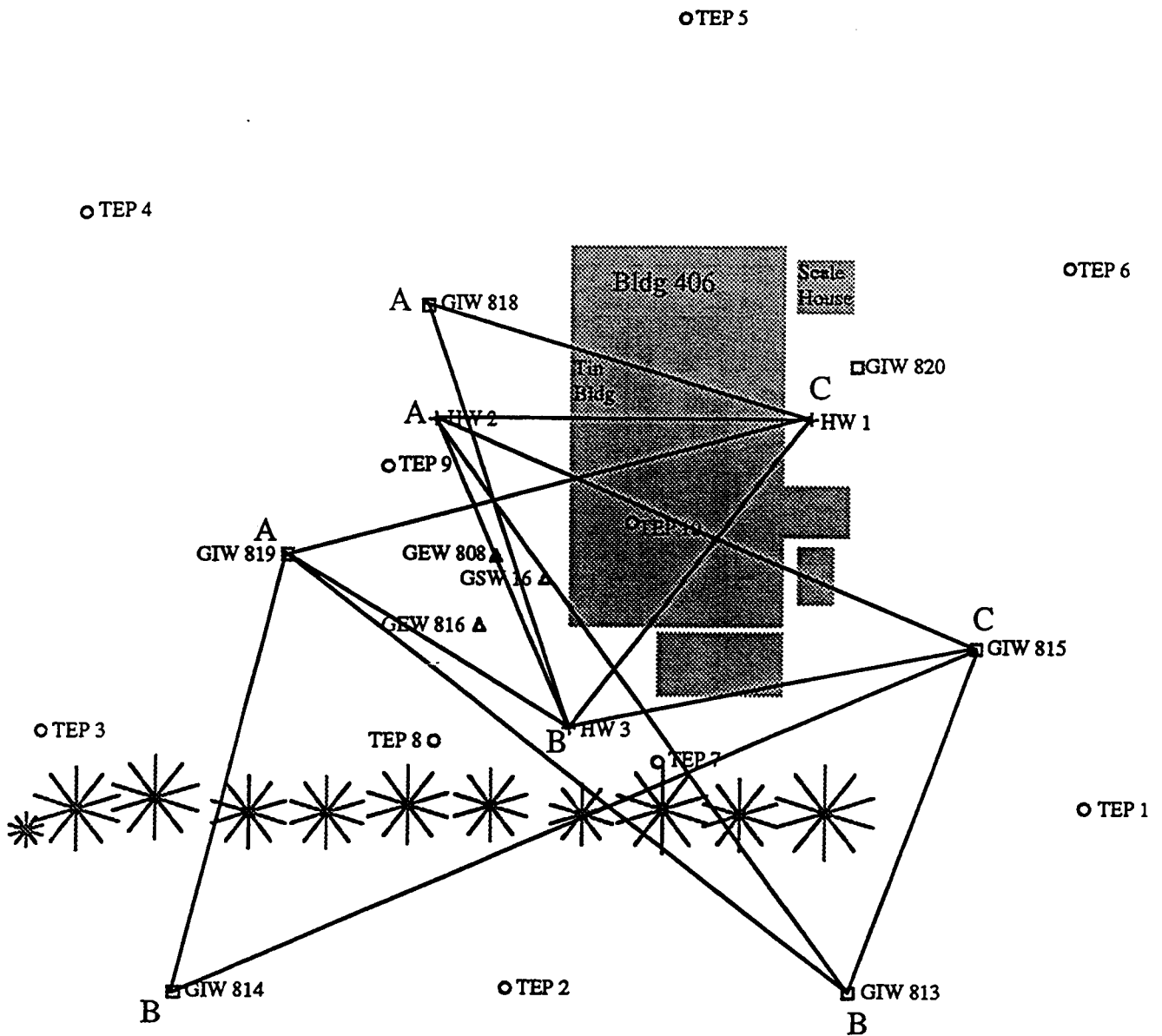
1 inch = 30 feet



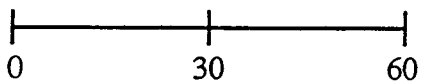
○ TEP 11

Fig. 5

Dynamic Stripping Project Gas Pad Area



Phase assignments and primary current flow paths
for alternate electrical heating configuration, Nov 24
to Dec 1 '92



1 inch = 30 feet

Well Types	
○	Monitoring Well
□	Injection Well
+	Heating Well
Δ	Extraction Well

○ TEP 11

Fig. 6

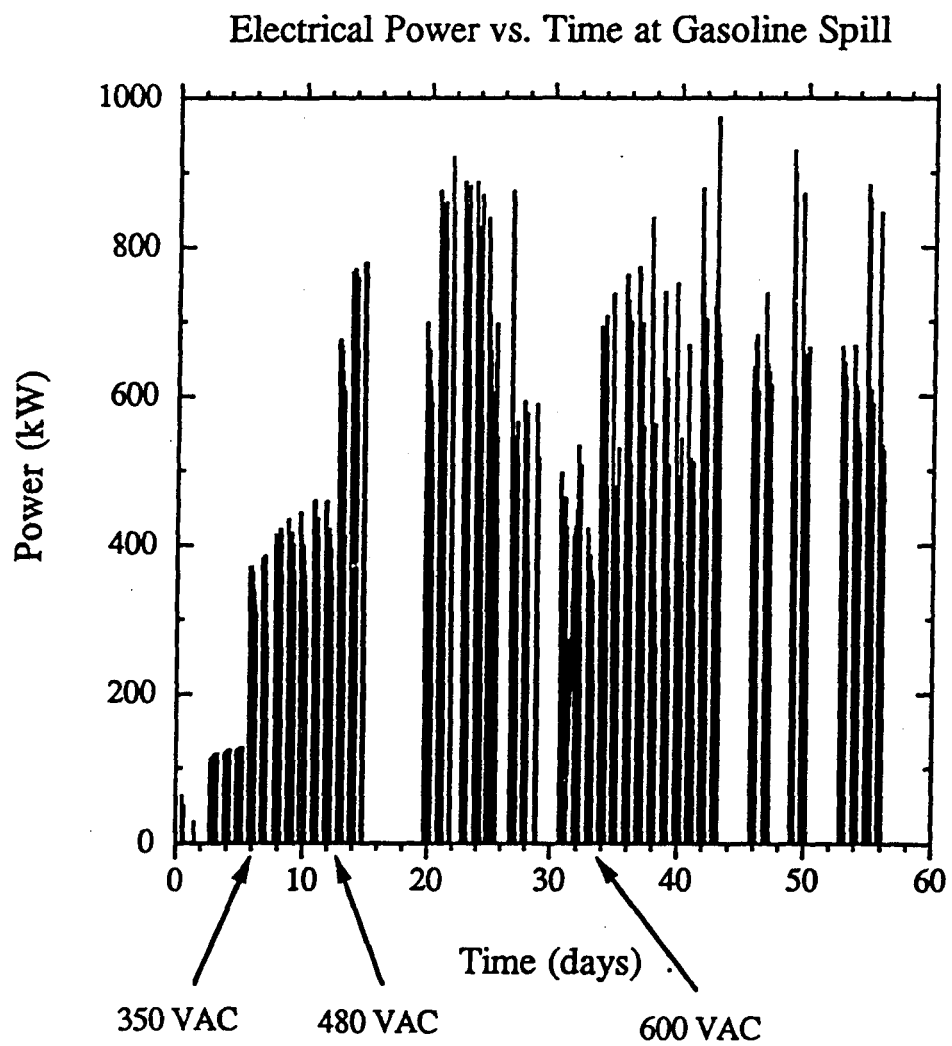


Fig. 7

Total Energy vs. Time at Gasoline Spill

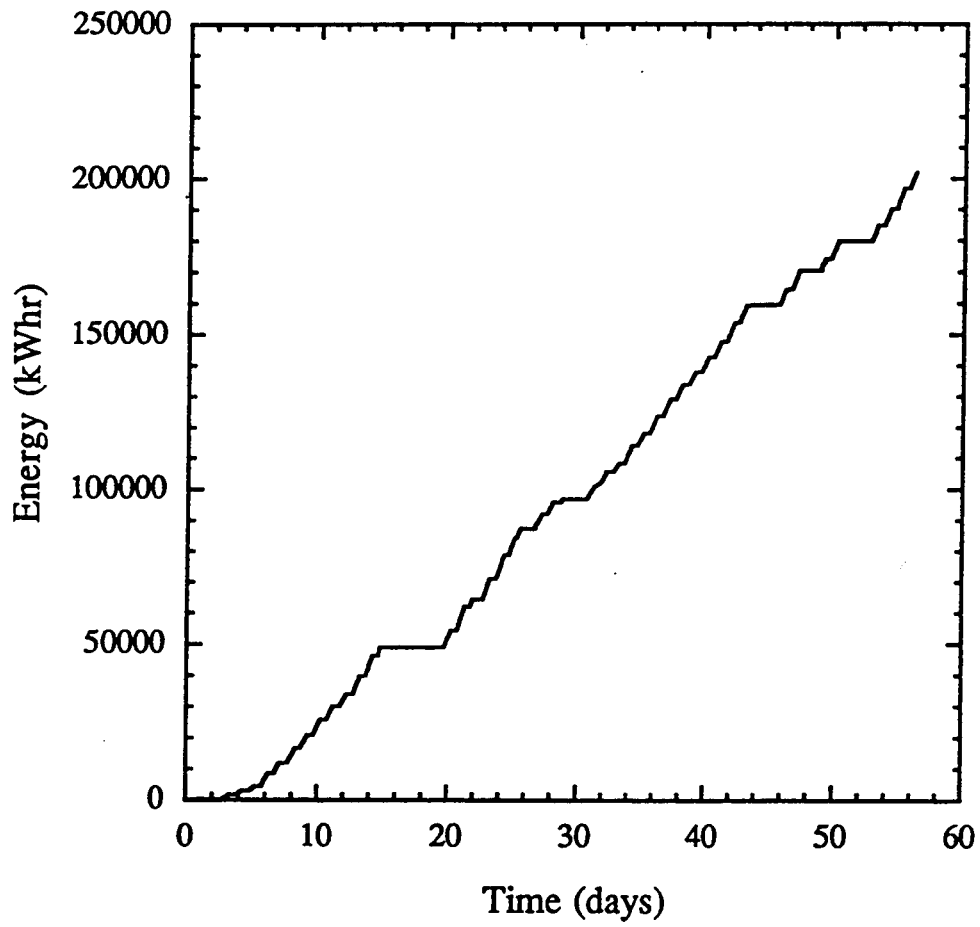


Fig. 8

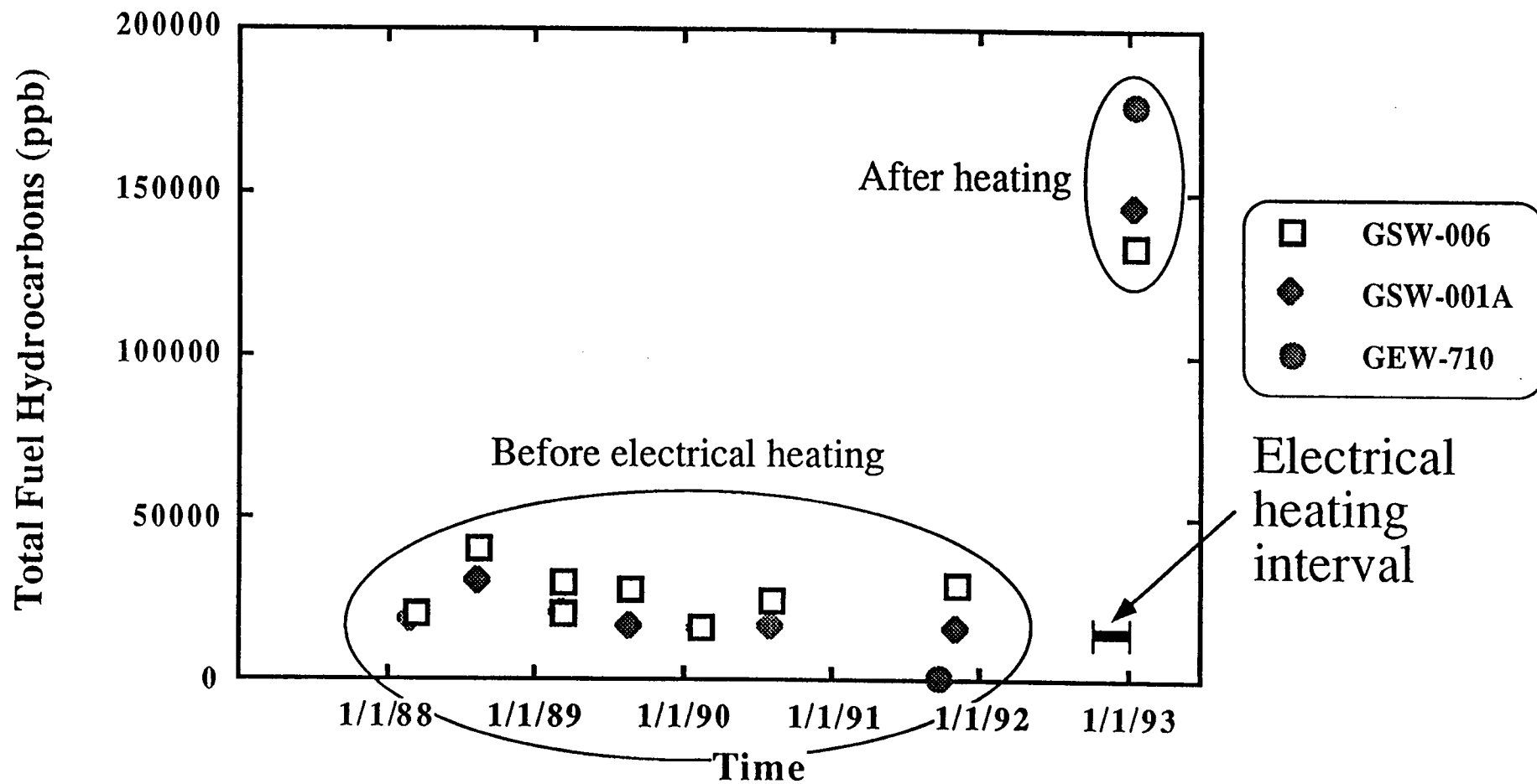
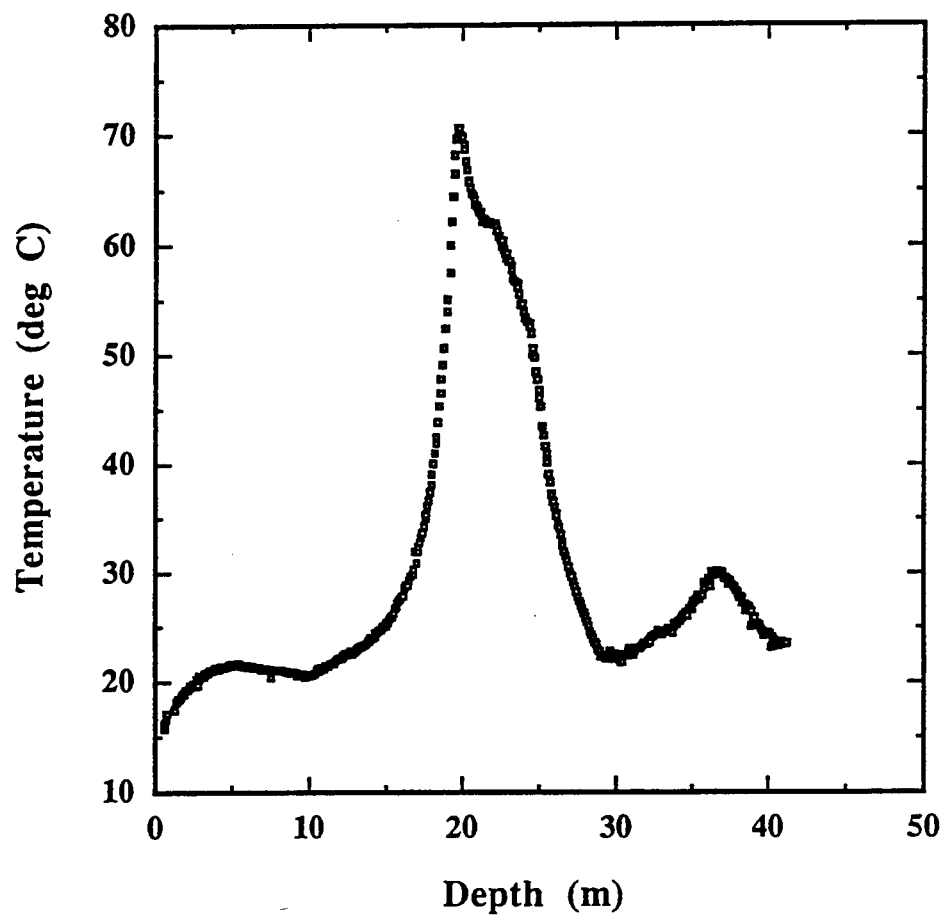
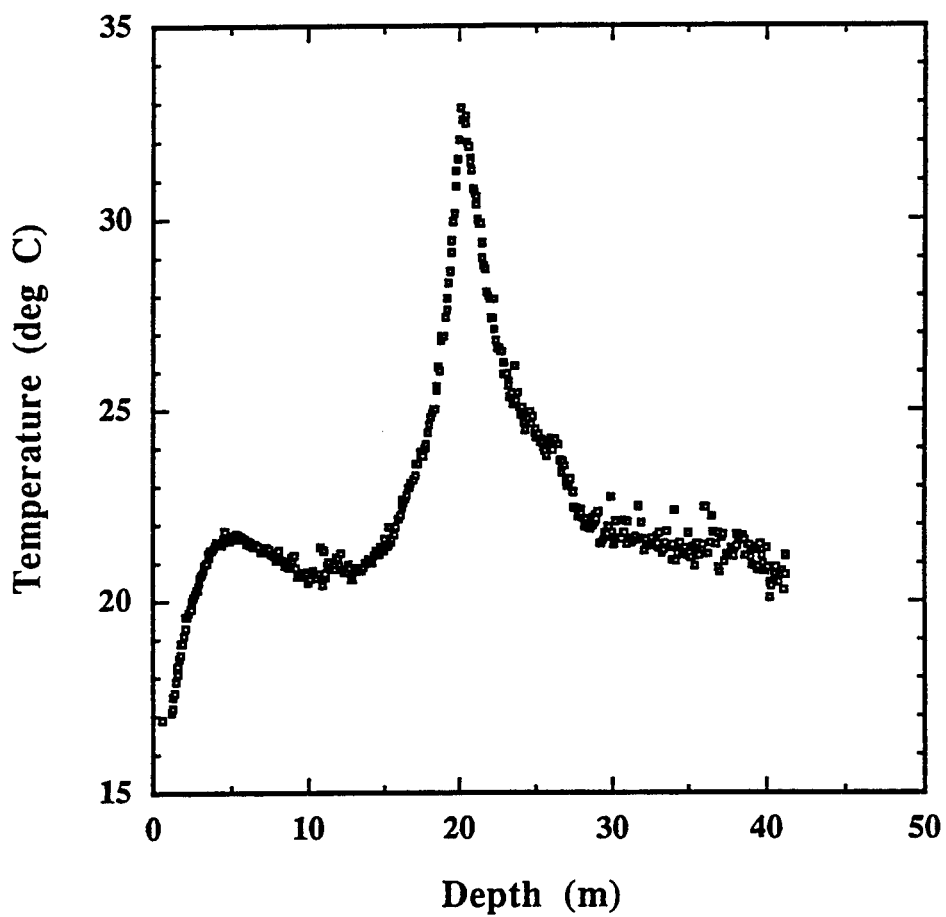


Fig. 9



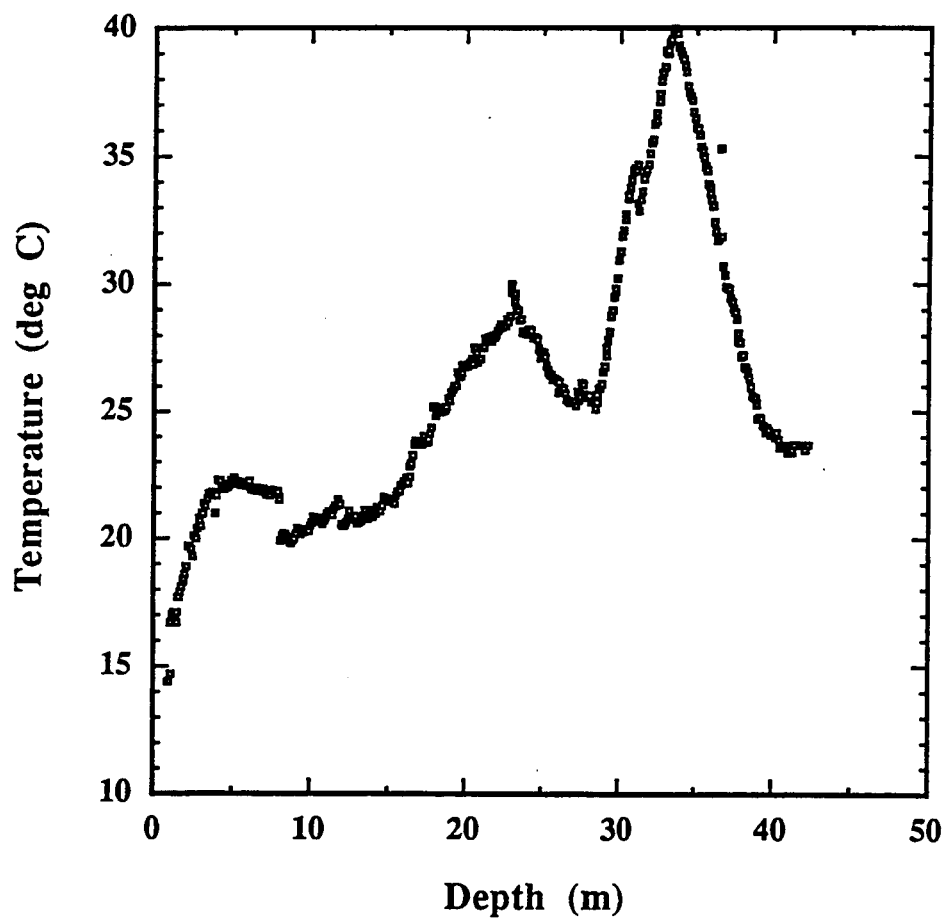
Temperature profile in well TEP 7 at the end of electrical heating.

Fig. 10



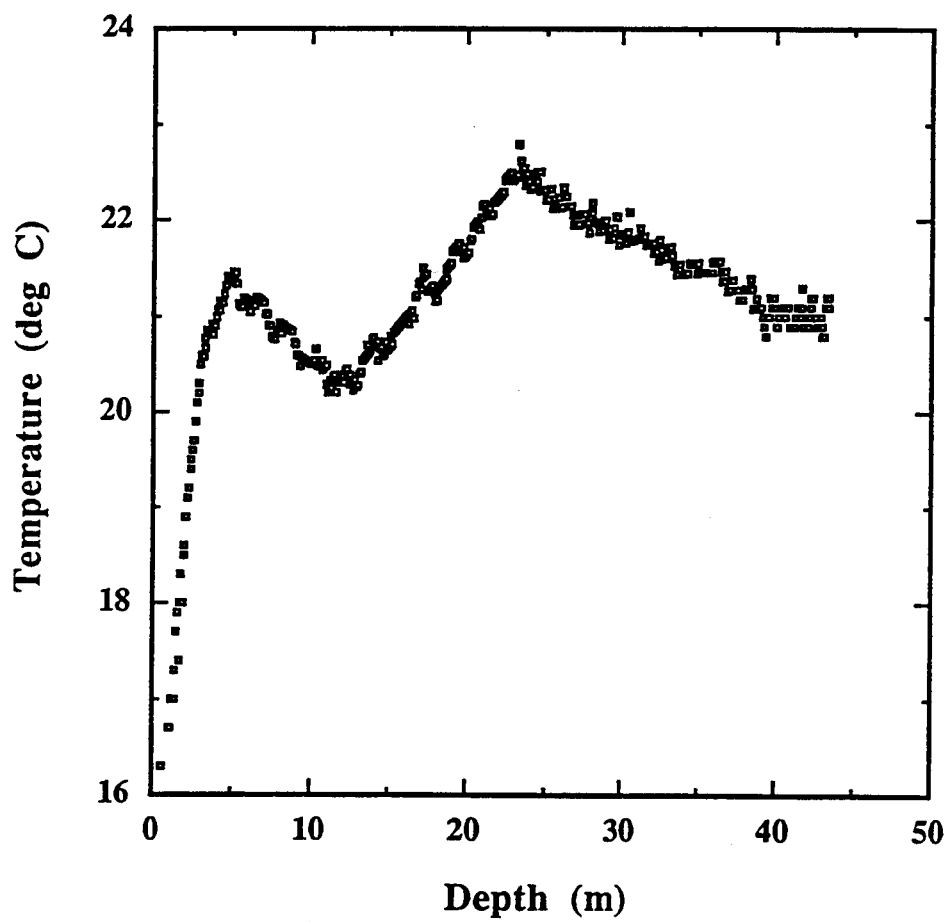
Temperature profile in well TEP 8 at the end of electrical heating.

Fig. 11



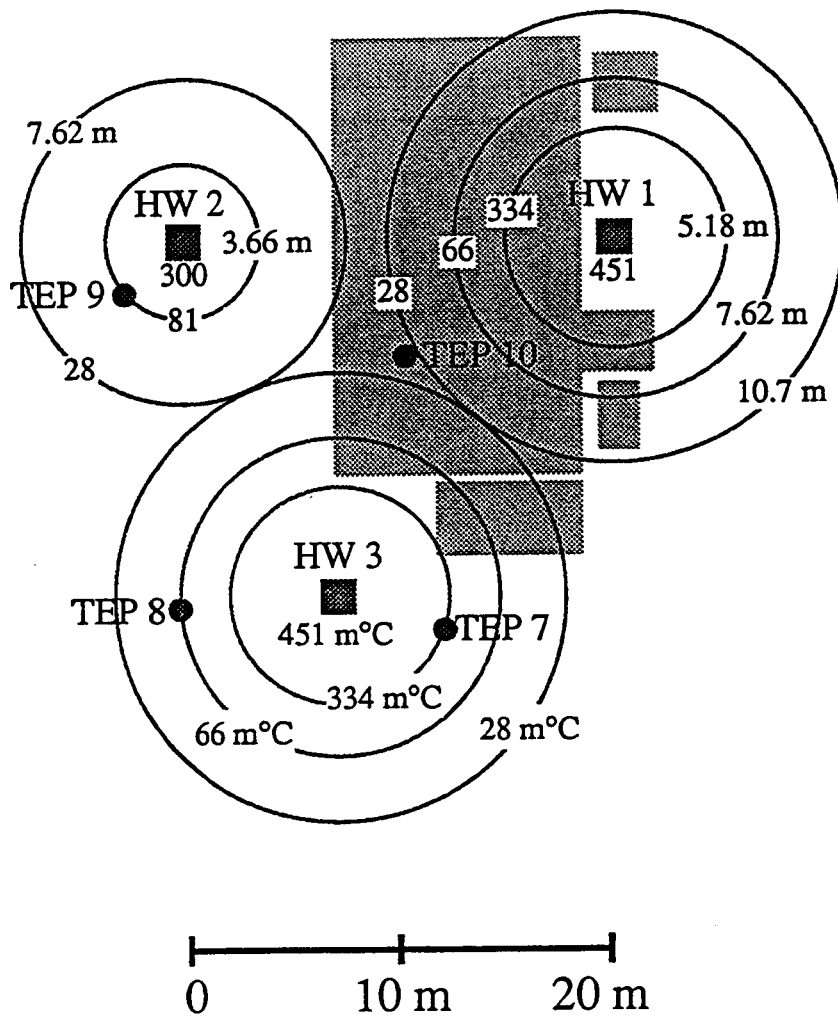
Temperature profile in well TEP 9 at the end of electrical heating.

Fig. 12



Temperature profile in well TEP 10 at the end of electrical heating.

Fig. 13



Plan view of upper zone heating wells with estimates of distance-temperature product and circles of influence.

Fig. 14

Appendix A

The Relative Importance of Joule and Conduction Heating

In the body of the report only joule heating was examined because it was assumed that joule heating would dominate conduction heating. This can be made more quantitative by comparing the relative importance of the joule heating term to the conduction heating term. Thus recall the heat equation

$$\frac{\partial T}{\partial t} = \frac{k}{cp} \nabla^2 T + \frac{U}{cp} \quad (A1)$$

and the joule heating source term

$$U = \sigma |\bar{E}|^2 \quad (A2)$$

When the current is first turned on, the temperature will vary linearly with time because the Laplacian of the initial temperature distribution is zero, and thus

$$T = T_0 + \frac{U}{cp} \Delta t \quad (A3)$$

where T is the temperature at the end of the time interval Δt and T_0 is the initial temperature distribution (assumed constant). Clearly the new temperature distribution depends on time and the spatial coordinates because the joule heating term varies spatially.

If one solved Equation (A1) by stepping along in time, the initial temperature would be T_0 everywhere, and at the end of the first time step Δt , the temperature would be given by Equation (A3). From Equation (A1), the rate of change of temperature at the end of the first time step would be given by

$$\frac{\partial T}{\partial t} = \frac{k}{cp} \frac{\sigma \Delta t}{cp} \nabla^2 |\bar{E}|^2 + \frac{\sigma |\bar{E}|^2}{cp} \quad (A4)$$

So, at the end of the first time step, the rate of change of the temperature is equal to the sum of the joule heating term (which varies as the square of the electric field) and the conduction term (which varies as the Laplacian of the square of the field). The joule heating term can now be compared to the conduction term to arrive at an estimate of when conduction becomes comparable to joule heating. Thus equating the two terms on the right hand side of A4 gives

$$\Delta t = \frac{cp|\bar{E}|^2}{k\nabla^2|\bar{E}|^2} \quad (A5)$$

Equation (A5) indicates that, for a given spatial distribution of electric field and thermal properties and at some particular location, there is a time interval Δt during which the heating will be dominated by joule heating. For times greater than this both terms will be important. In fact, even if the current is turned off, there can still be significant heating by conduction provided enough time has elapsed.

For purposes of illustration, consider the simple case of heating from a line source of current. This two-dimensional case corresponds to that of a line electrode embedded in a conducting layer which is separated from other conducting layers by insulating layers. For example, the case of a clay layer with insulating gravels above and below, all of which are above the water table is well modeled by this case.

In the two-dimensional case the electric field is given by

$$|\bar{E}| = \frac{I}{2\pi\sigma r} \quad (A6)$$

where r is the radial distance from the line source of current. Thus the square of the field term is

$$|\bar{E}|^2 = \left(\frac{I}{2\pi\sigma r} \right)^2 \quad (A7)$$

With variations in r only, the Laplacian is given by

$$\nabla^2 = \frac{1}{r} \frac{d}{dr} \left(r \frac{d}{dr} \right) \quad (\text{A8})$$

and thus

$$\nabla^2 |\bar{E}|^2 = \left(\frac{I}{\pi \sigma} \right)^2 r^{-4} \quad (\text{A9})$$

and substitution of A7 and A9 into A5 yields

$$\Delta t = \frac{cpr^2}{4k} \quad (\text{A10})$$

Substitution of some typical values of the thermal properties of soils into Equation (A10) allows for an estimate of the time Δt . Values of cp and k from Carslaw and Jaeger for average soil, namely $cp = 2 \times 10^6$ joule/m³·°C and $k = 1$ W/m·°C. Thus

$$\Delta t = 5 \times 10^5 r^2 \quad (\text{A11})$$

For example, at a distance of 1 meter, Δt is 5×10^5 seconds or 5.79 days, at 2 meters, the time is 23.1 days, at 3 meters the time is 52.1 days, and finally at 10 meters, it is 579 days.

These calculations have important implications for the design of an electrical heating-assisted vacuum venting cleanup. For example, in a remediation scenario where the heating is to take place over two months, conduction heating will not be significant unless the area to be heated is less than about 3 m from a heating electrode. If, however, the time frame is extended to 18 months, then the electrodes could be as much as 10 m from the region to be heated.

This analysis has neglected the effects of heterogeneous soil properties and the benefits of using arrays of heating electrodes rather than one, but the basic conclusions should still be valid.

Appendix B

Time History of Energy Deposition for Individual Electrodes

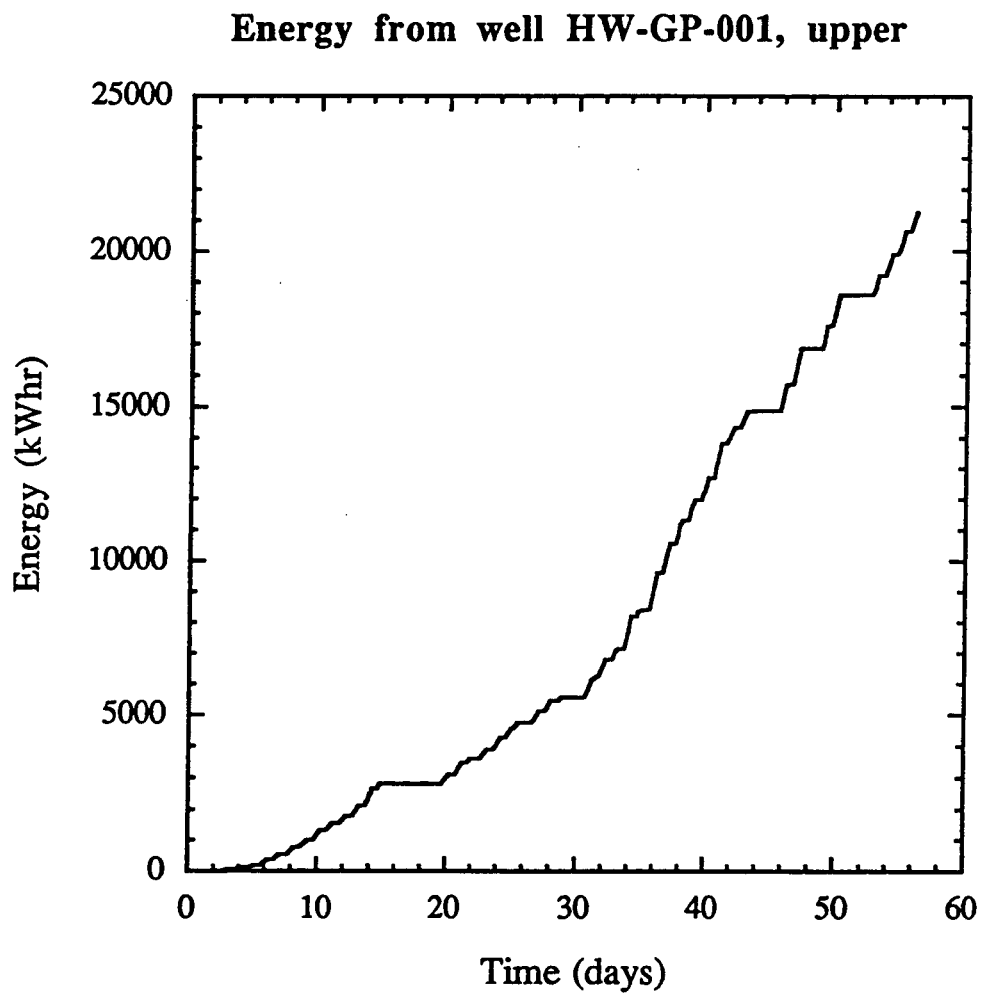


Fig. B-1

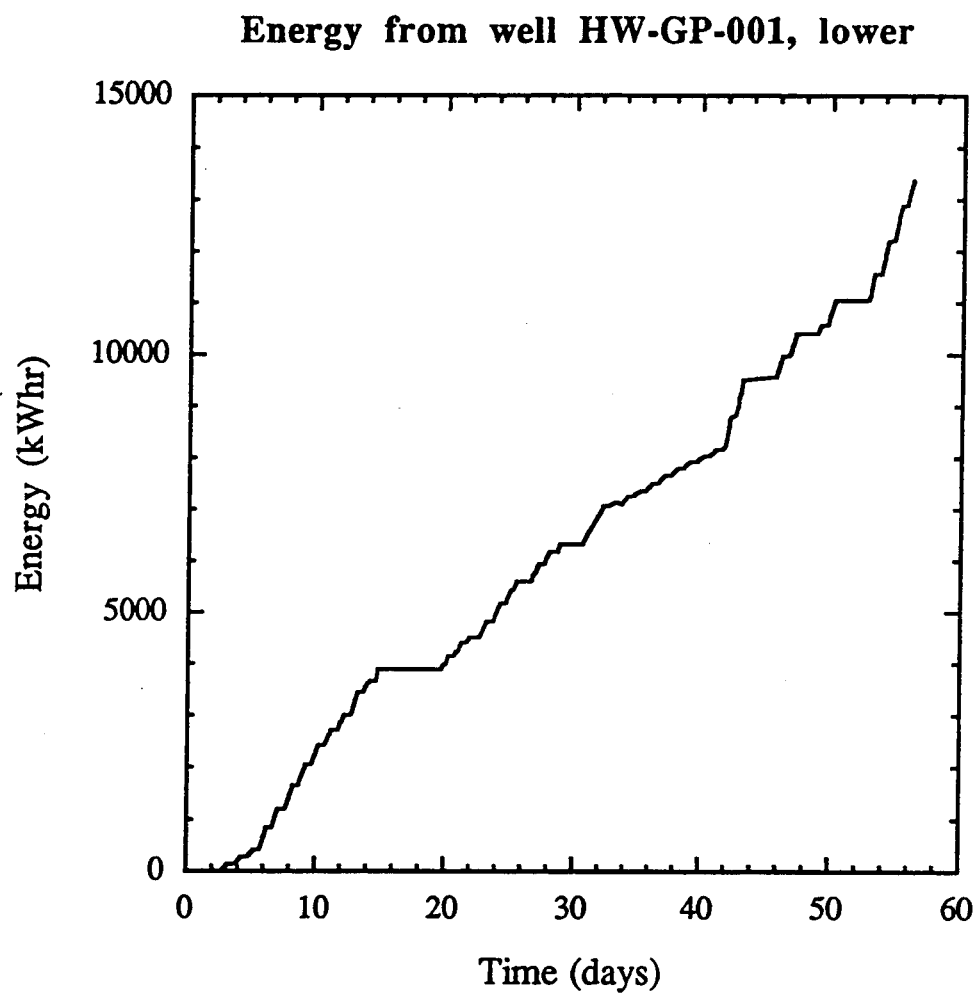


Fig. B-2

Energy from well HW-GP-002, upper

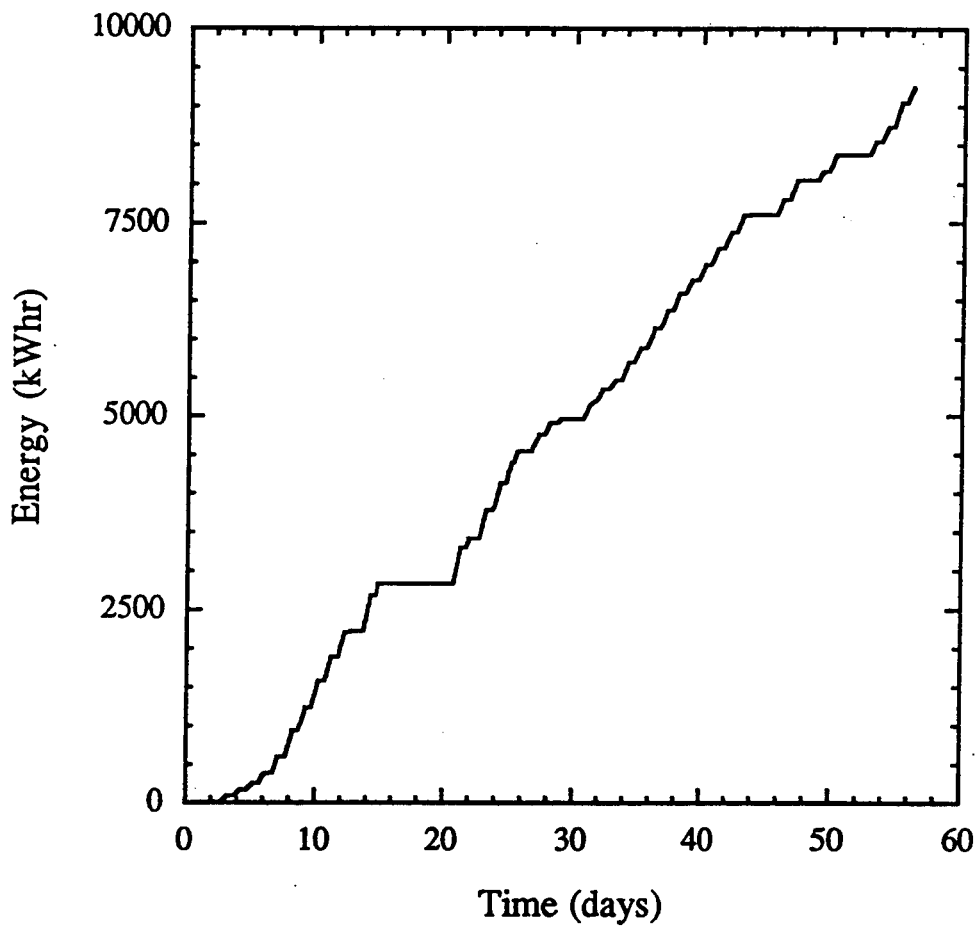


Fig. B-3

Energy from well HW-GP-002, lower

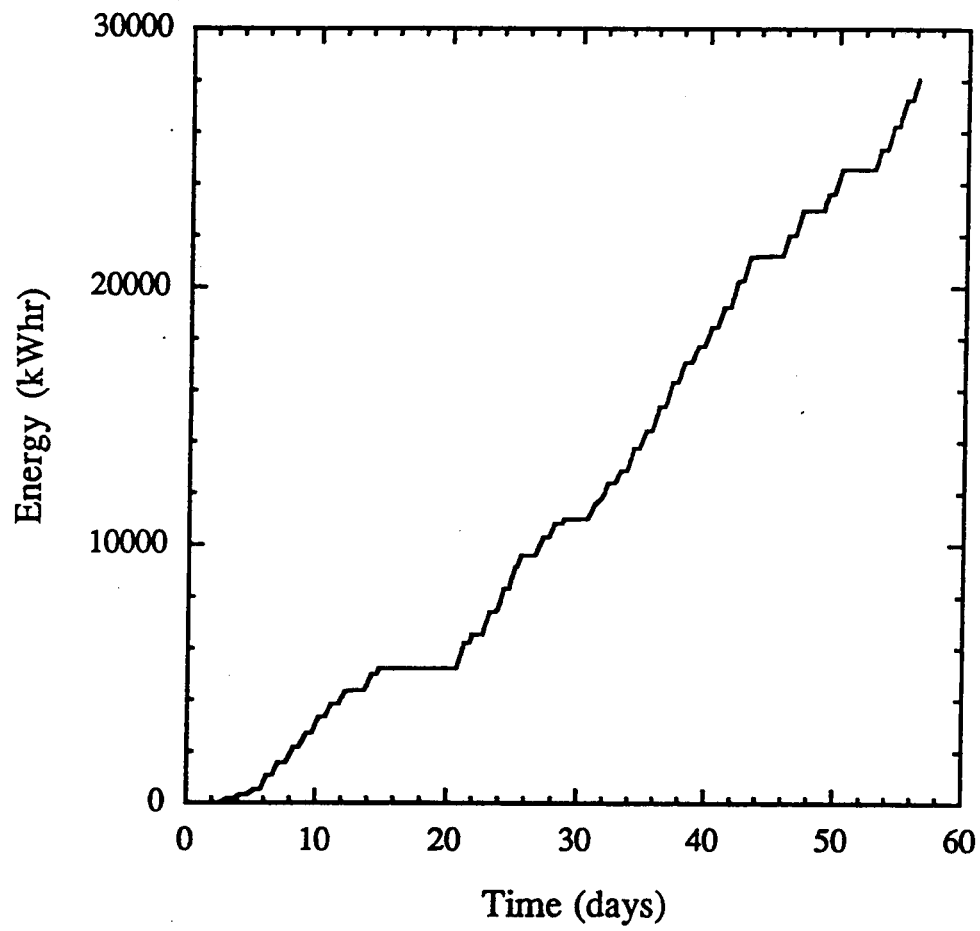


Fig. B-4

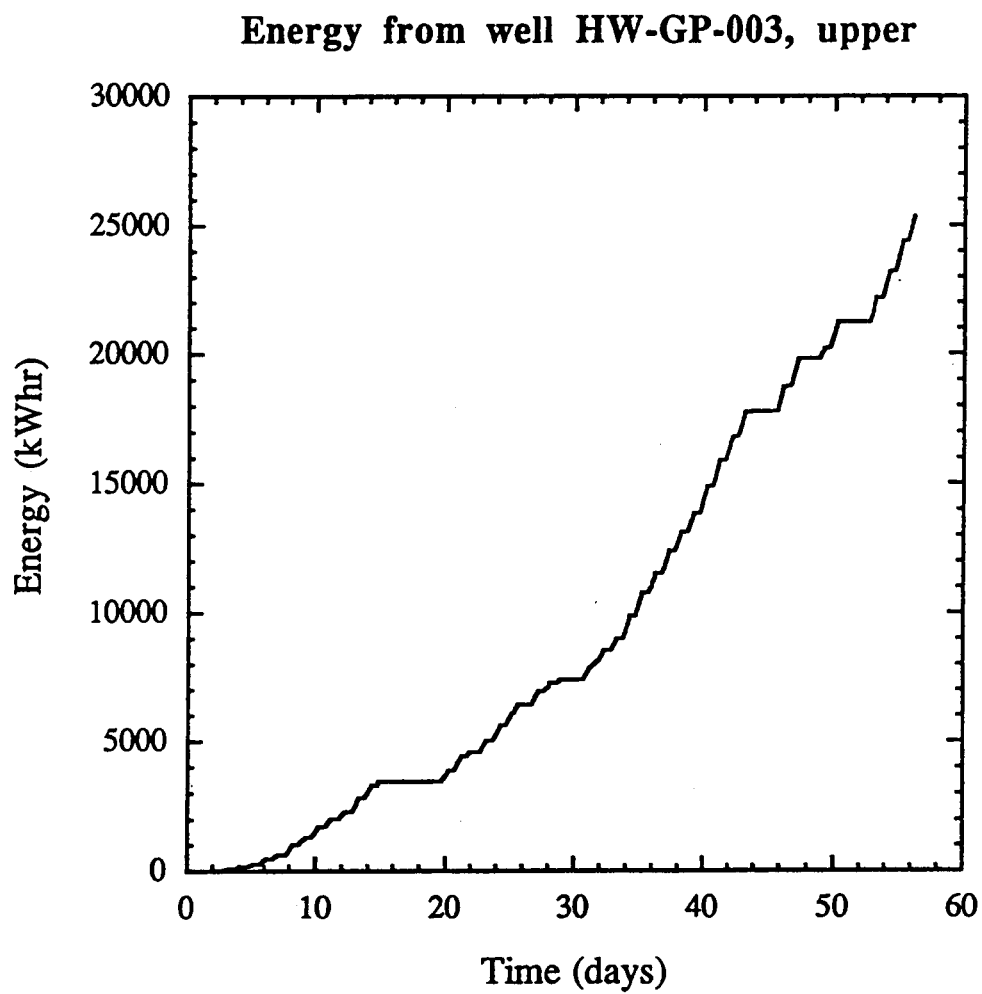


Fig. B-5

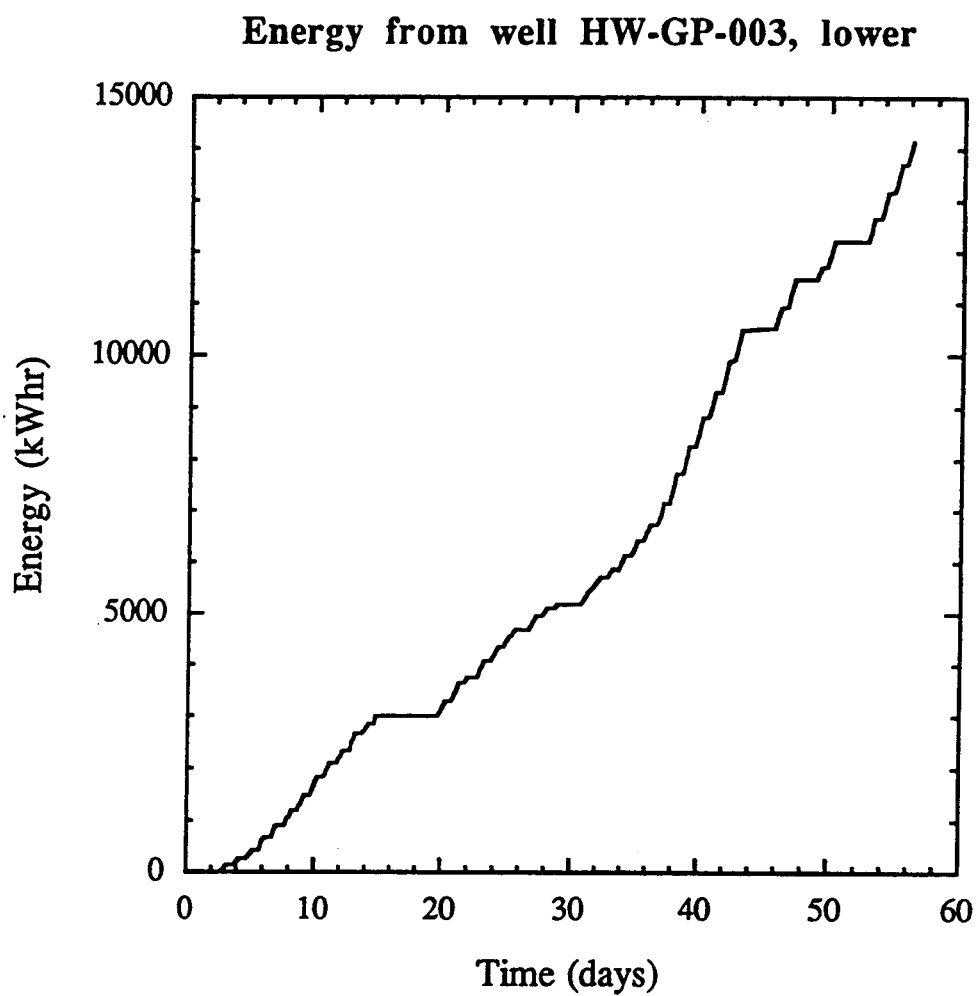


Fig. B-6

Energy from well GIW-813

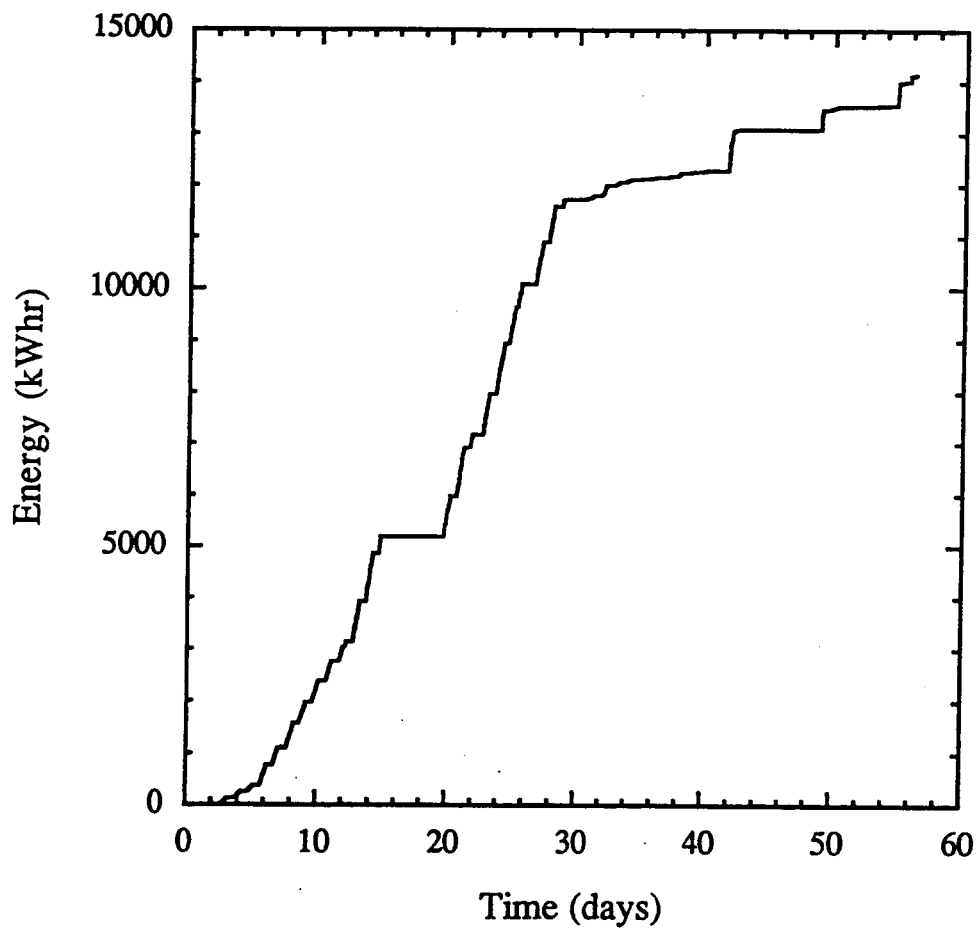


Fig. B-7

Energy from well GIW-814

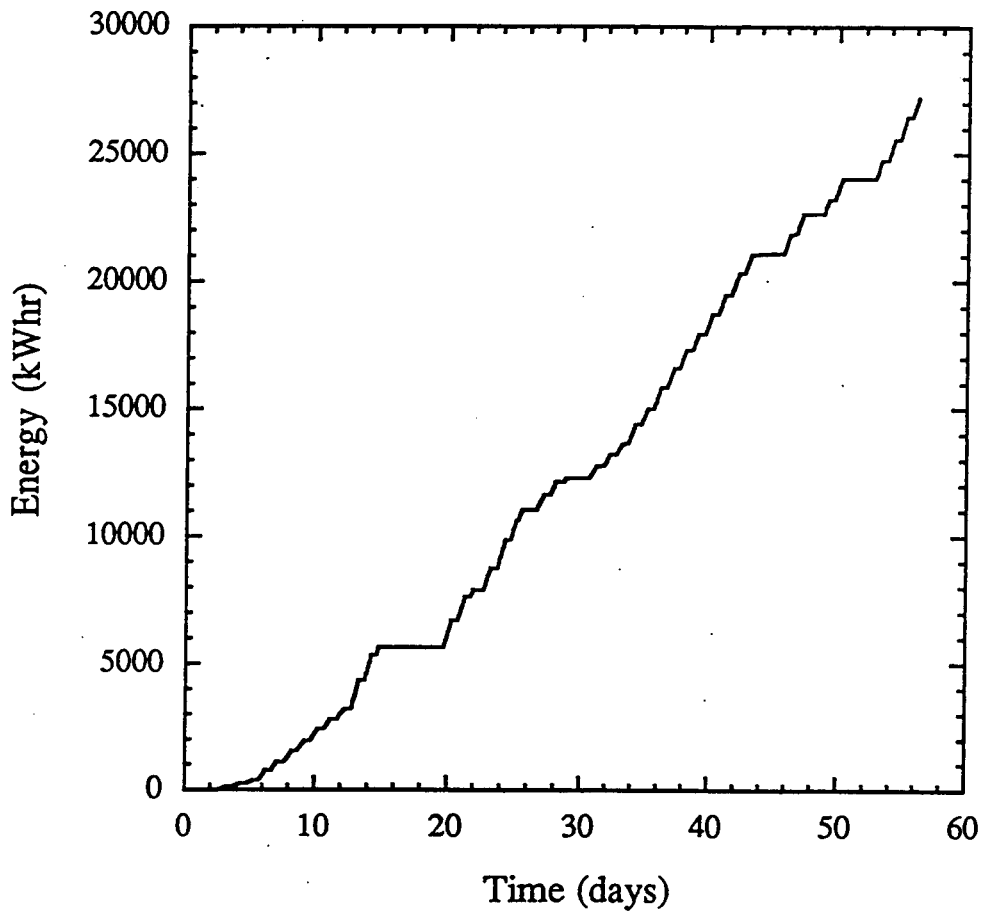


Fig. B-8

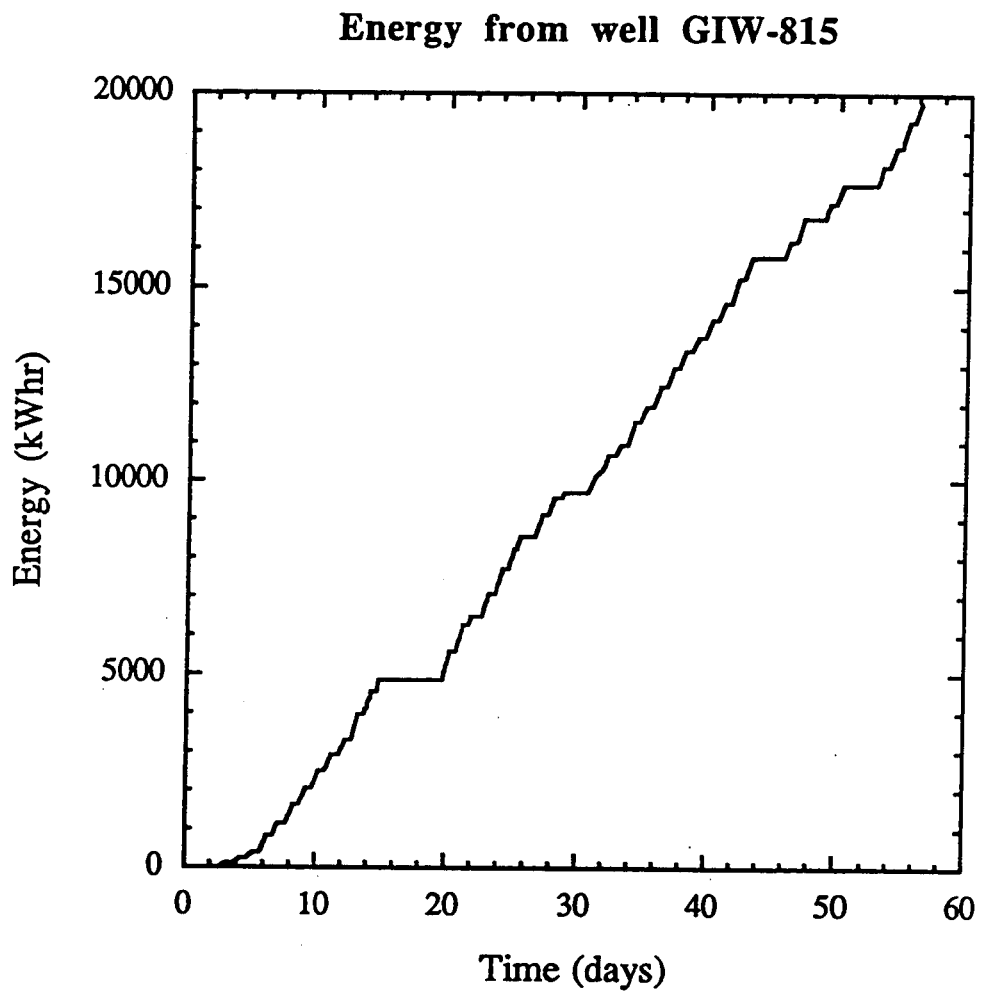


Fig. B-9

Energy from well GIW-818

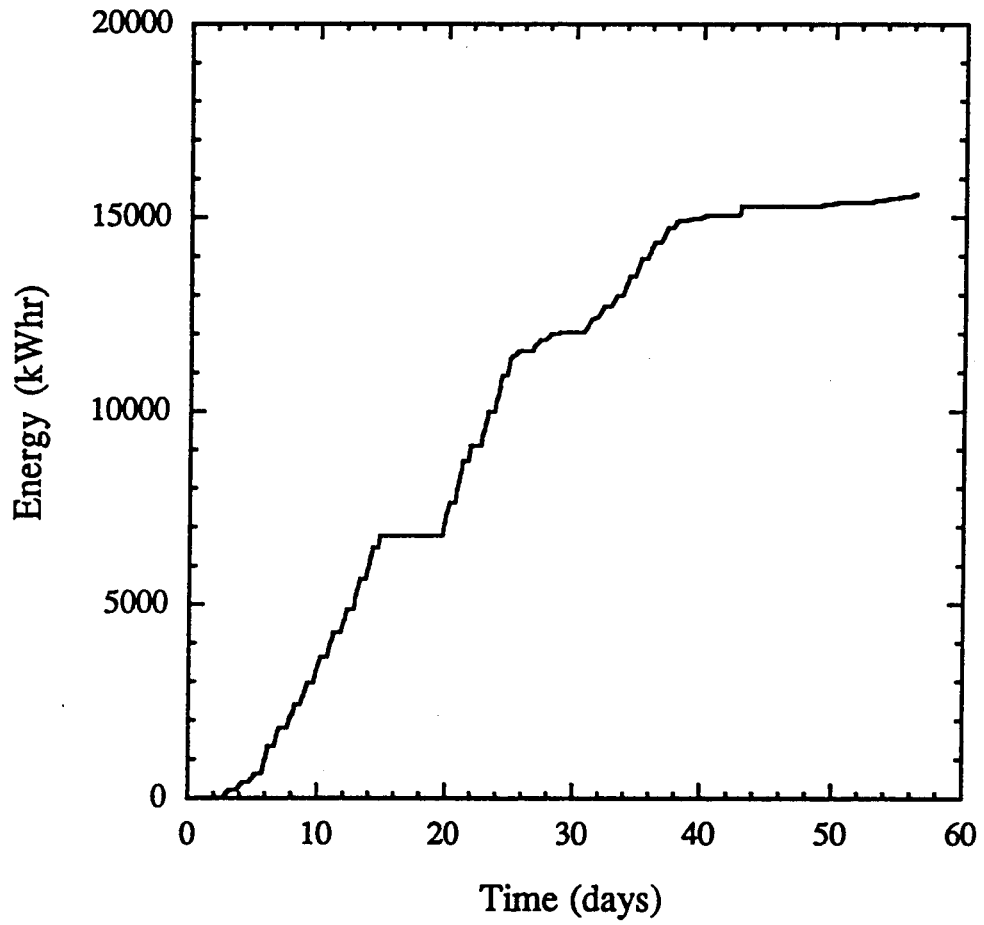


Fig. B-10

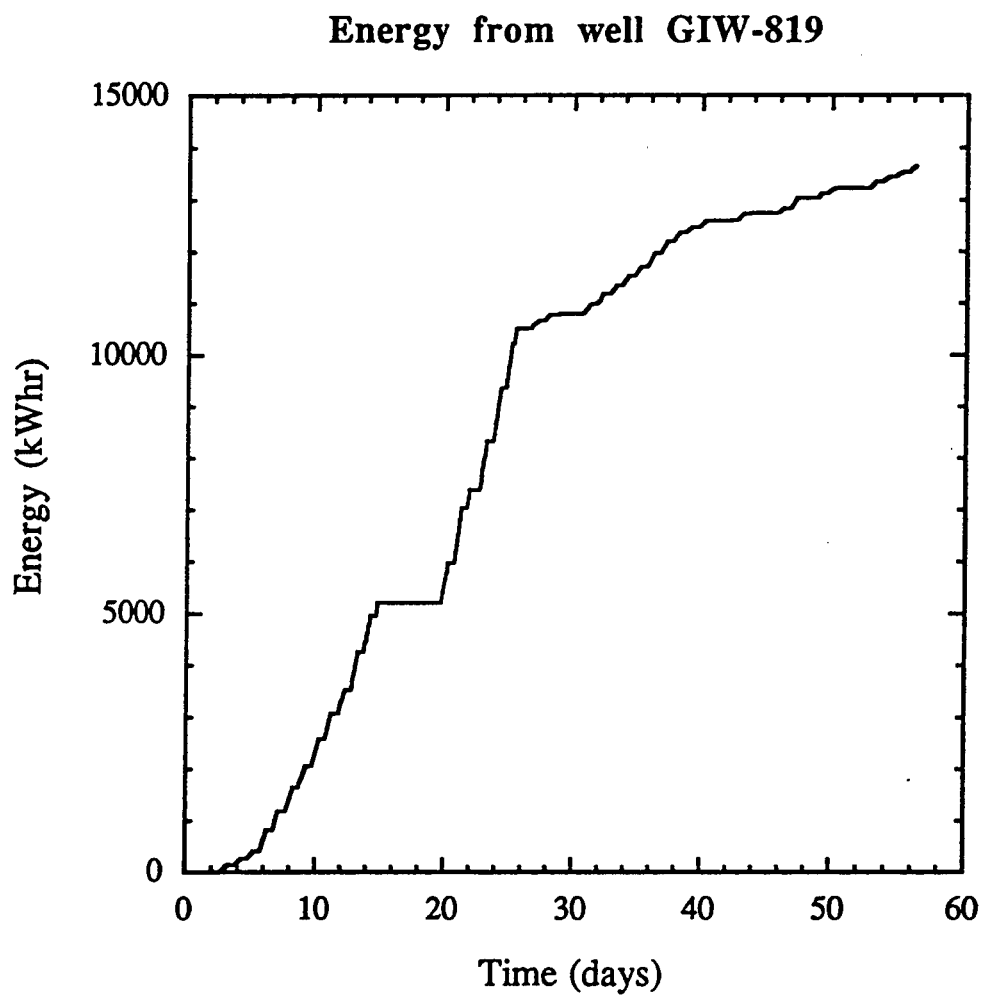


Fig. B-11